Fuel 390 (2025) 134725

Contents lists available at ScienceDirect

Fuel

journal homepage: www.elsevier.com/locate/fuel

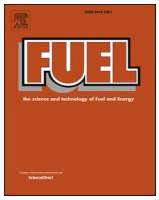

Full Length Article

The effect of TiO_2 nanoadditive on emissions, exergetic performance, and enviro/social/economic indicators in a small UAV jet engine fuelled with kerosene

Usame Demir [a,*], Halil Erdi Gülcan [b], Salih Özer [c]

[a] Department of Mechanical Engineering, Bilecik Şeyh Edebali University, Bilecik, Turkey
[b] Department of Mechanical Engineering, Faculty of Technology, Selcuk University, Konya, Turkey
[c] Department of Mechanical Engineering, Muş Alparslan University, Muş, Turkey

ARTICLE INFO

Keywords:
Jet engine emissions
Energy and exergy analysis
Environmental analysis
Economic analysis
TiO_2 nanoadditive

ABSTRACT

The vehicles used in the aviation sector are widely employed in both transportation and industrial fields, and the energy requirements of these tools are currently met with fossil-based fuels. Reducing the consumption of these fossil fuels could contribute to mitigating environmental and economic impacts. Nanoparticle additives can be used in fossil-derived fuels to reduce fuel consumption. In this study, the effects of adding different proportions of TiO_2 nanoparticles to kerosene (Jet A1) fuel in a jet engine are examined from the perspectives of performance, emissions, energy, exergy, and environmental-economic impacts. The experiments are conducted with three different test fuels (Jet A1, Jet A1+100 ppm TiO_2, and Jet A1+200 ppm TiO_2) and at nine different engine speeds (from 40 k rpm to 120 k rpm in increments of 10 k rpm). The results demonstrate that the use of TiO_2 (200 ppm) in Jet A1 fuel reduced specific fuel consumption by an average of 16 % and decreased HC, CO, and CO_2 emissions by average percentages of 18 %, 17 %, and 10 %, respectively. Additionally, the exergy efficiencies of the compressor, combustion chamber, and gas turbine systems were found to increase with TiO_2 usage. Moreover, the addition of TiO_2 to Jet A1 fuel showed the potential to reduce enviroeconomic impact by up to 10 %. In conclusion, it can be stated that the use of TiO_2 in Jet A1 fuel is beneficial for reducing fuel consumption, enhancing exergetic efficiency, and improving enviroeconomic sustainability of jet engines used in both industrial and transportation sectors.

1. Introduction

The increasing global demand for energy and the associated environmental concerns have intensified the search for sustainable and efficient fuel alternatives, particularly in the aviation sector [1]. The aviation sector is expected to experience a substantial shortage of jet fuel by 2026 due to the predicted decline in crude oil production, necessitating the development of alternative fuels to meet growing demand [2]. This synthesis examines the potential of various alternative fuels and technologies to meet the aviation industry's energy needs while addressing environmental impacts [3]. Recent developments in low-carbon aviation fuel (LCAF) and sustainable aviation fuel (SAF) have shown potential to improve the sustainability of the aviation sector [4]. In recent years, the biodiesel production methods used in sustainable aviation fuels have also been discussed, and they have entered the literature as methods that provide high conversion efficiency [5,6]. Despite these methods, it is anticipated that SAF fuels will not be sufficient under current conditions. These fuels can reduce greenhouse gas emissions and are considered a viable alternative to fossil-based fuels [7]. Synthetic fuels, derived from various feedstocks, offer a potential alternative to petroleum-based jet fuels [8,7,9]. However, economic costs and feedstock availability are significant barriers to their near-term adoption in aviation [10]. Despite the push for alternative fuels, internal combustion engines (ICEs) will continue to dominate commercial transport for the foreseeable future [11–13]. Improvements in ICE technology, such as gasoline compression ignition (GCI) and octane on demand (OOD), can enhance fuel efficiency and reduce emissions [14,15]. Bio-aviation fuels can be produced from various biomass sources, such as castor oil [16], jatropha [17], and palm kernel oils [18], achieving high yields and meeting quality standards when blended with conventional jet [19,20]. The increasing global demand for energy and

* Corresponding author.
E-mail address: usame.demir@bilecik.edu.tr (U. Demir).

https://doi.org/10.1016/j.fuel.2025.134725
Received 19 November 2024; Received in revised form 5 February 2025; Accepted 12 February 2025
Available online 19 February 2025

Nomenclature

cf	Compressibility fraction
c_p	Specific heat at constant pressure, (k J/kgK)
$\dot{E}n_{in}$	Energy input, (k W)
$\dot{E}n_f$	Fuel energy, (k W)
Env_{eco}	Environmental cost, (Euro/kNh)
Env_{im}	Environmental impact, (mPts/kNh)
Env_{sc}	Enviro-social cost, (Euro/kNh)
$\dot{E}x_{in}$	Exergy input, (k W)
$\dot{E}x_{Dest.}$	Exergy destruction, (k W)
$\dot{E}x_{D,C}$	Compressor exergy destruction, (k W)
$\dot{E}x_{D,CC}$	Combustion chamber exergy destruction, (k W)
$\dot{E}x_{D,GT}$	Gas turbine exergy destruction, (k W)
$\dot{E}x_f$	Fuel exergy, (k W)
$\dot{E}x_{ph}$	Physical exergy, (k W)
$\dot{E}n_{out}$	Energy output, (k W)
$\dot{E}x_{out}$	Exergy output, (k W)
$\dot{m}_{air}$	Mass flow of air, (k g/h)
$\dot{m}_{fuel}$	Mass flow of fuel, (k g/h)
$\dot{m}_{gas}$	Mass flow of combustion products, (kg/h)
Q_f	Lower heating value of the fuel, (kJ/kg)
Q_{loss}	Heat loss, (kW)
$\overline{R}$	Universal gas constant, (kJ/kmolK)
$\dot{W}_{Comp}$	Compressor work, (kW)
$\dot{W}_{GT}$	Gas turbine work, kW
T_0	Ambient temperature, (K)
T_1	Ambient temperature, (K)
T_2	Compressor outlet temperature, (K)
T_3	Combustion temperature, (K)
T_4	Gas turbine outlet temperature, (K)
ψ	Exergy efficiency
φ_{fuel}	Chemical exergy factor of fuel

the associated environmental concerns have intensified the search for sustainable and efficient fuel alternatives, particularly in the aviation sector [21]. Jet A1 fuel, a kerosene-based aviation fuel, is the predominant choice due to its high energy content, stability, and widespread availability [22]. However, the combustion of Jet A1 fuel in jet engines produces significant emissions of hydrocarbons (HC), carbon monoxide (CO), and carbon dioxide (CO_2), all of which contribute to air pollution and climate change [23]. Reducing these emissions while maintaining or improving fuel efficiency is a critical challenge for the aviation industry [24].

Nanotechnology offers a promising approach to enhancing fuel properties and performance [25,26]. Titanium dioxide (TiO_2) nanoparticles, known for their catalytic properties and high surface area-to-volume ratio, have shown the potential to improve combustion efficiency and reduce hydrocarbon-based fuel emissions [27,28]. Studies on diesel and gasoline fuels have demonstrated that TiO_2 nanoparticles can enhance fuel performance, increase energy efficiency, and decrease harmful emissions [29,30]. Recent studies have highlighted the role of nanoparticle additives in improving fuel performance, emissions reduction, and thermal management in energy systems, further underscoring their potential in aviation fuels [31–35]. Despite these promising findings, there is limited research on the effects of TiO_2 nanoparticles when added to Jet A1 fuel, particularly in the context of jet engines.TiO_2 nano additives have been shown to reduce emissions in various engines significantly. For instance, TiO_2 reduced CO, HC, and smoke emissions in diesel engines while improving overall combustion efficiency [36]. Similar reductions were observed in other studies where TiO_2 was added to different fuel blends [37]. Notably, adding TiO_2 to fuels reduced CO and HC emissions and decreased NOx emissions in some cases, although it could increase NO_x in others depending on the specific engine and operational conditions [38].

Studies show that adding TiO_2 to fuels enhances exergetic efficiency, meaning the fuel is used more effectively for energy production, reducing waste and increasing overall engine efficiency [39]. This improvement in efficiency often translates to better engine performance, with increases in power output and reductions in specific fuel consumption observed in engines running on TiO_2-enhanced fuels [40]. Reducing harmful emissions (such as CO, HC, and NO_x) contributes positively to environmental sustainability by decreasing the environmental footprint of UAV operations [41]. Economically, the increased fuel efficiency and reduced wear and tear on engines due to cleaner combustion can lower operating costs over time [42].

The use of TiO_2 nanoadditives in kerosene-fueled UAV jet engines can significantly improve emissions profiles and exergetic performance, with positive implications for environmental sustainability and economic efficiency. These benefits highlight the potential of TiO_2 as a valuable additive in aerospace applications.

In conclusion, this study investigates the effects of TiO_2 nanoparticles as additives to Jet A1 fuel on the performance and emissions of a UAV jet engine. The central research hypothesis posits that including TiO_2 nanoparticles at specific concentrations improves combustion efficiency, reduces emissions, and enhances jet engine operations' environmental and economic sustainability. This hypothesis stems from the urgent need to address the challenges of reducing aviation's carbon footprint associated with fossil-based fuels, aligning directly with global sustainability goals in the aerospace sector.

The significance of this research in its contribution to the environmental-economic nexus, demonstrating how nanoparticle-enhanced fuels can simultaneously lower harmful emissions (such as CO, HC, and CO_2) and improve fuel efficiency, thereby reducing overall fuel consumption costs. Such advancements offer potential operational savings for the aviation industry and support compliance with increasingly stringent environmental regulations. The findings aim to provide a pathway for balancing ecological responsibility with economic viability, ensuring the broader adoption of sustainable fuel technologies.

The novelty of this work in its exploration of TiO_2 nanoparticle additives in the context of jet engines, a relatively underexplored area compared to their use in diesel and gasoline engines. By systematically analyzing the effects of varying TiO_2 concentrations across various engine speeds, this study provides the first comprehensive evaluation of the operational, environmental, and economic impacts of nano-enhanced Jet A1 fuel on UAV jet engines. These results lay the groundwork for further exploration of nanoparticle-enhanced fuel technologies, potentially influencing regulatory standards and supporting the aviation industry's transition toward more sustainable energy solutions.

2. Material and method

The primary fuel used in this study is Jet A1, a standard kerosene-based aviation fuel. Titanium dioxide (TiO_2) nanoparticles were used as additives. These nanoparticles were procured in high-purity form to ensure consistent quality and performance.

The primary fuel used in this study is Jet A1, a standard kerosene-based aviation fuel. Titanium dioxide (TiO_2) nanoparticles were used as additives. These nanoparticles were procured in high-purity

commercial form to ensure consistent quality and performance. To provide a clearer understanding of the properties of the TiO_2 nanoparticles used in this study, their key characteristics are summarized in Table 1.

Three different of test fuels were prepared. These fuel mixtures are Pure Jet A1, Jet A1 with 100 parts per million (p pm) TiO_2 nanoparticles, and Jet A1 with 200 ppm TiO_2 nanoparticles. The physical properties of the prepared fuels can be seen in Table 2.

The TiO_2 nanoparticles were dispersed in Jet A1 fuel using an ultrasonic homogenizer to ensure uniform distribution. Adding the specified amount of TiO_2 nanoparticles to Jet A1 fuel. Ultrasonically agitating the mixture for 30 min at a frequency of 20 kHz to achieve a stable colloidal suspension.

The experiments were conducted using A JetCat P80-SE type small turbojet engine designed to simulate the operational conditions of commercial jet engines. The turbojet engine specifications included a maximum speed of 125,000 rpm and a thrust output suitable for laboratory-scale testing. An advanced engine control system was used to regulate engine speed and monitor performance parameters precisely. Turbojet engine specifications can be seen in Table 3.

Fig. 1 presents a schematic representation of the experimental test setup, where the symbols and colors indicate various components and their functions. The blue rectangles represent critical elements of the system, including the fuel tank located at the top-right, which stores the test fuels (Jet A1, Jet A1+100 ppm TiO_2, and Jet A1+200 ppm TiO_2), and the emission device on the left, which is responsible for analyzing the exhaust gases for key emissions such as CO, HC, CO_2, and NO_x. The green square in the center-right corresponds to the air inlet measurement system, which monitors the airflow entering the engine to ensure proper combustion. The main body of the turbojet engine is shown in red at the center, indicating the core system responsible for combustion, thrust generation, and exhaust. The red line connecting to the engine represents the ignition control line, which regulates the ignition process to ensure consistent combustion of the test fuels. Black lines are used to represent the critical connections, including the fuel line that transfers fuel from the storage tank to the engine, the motor speed measurement line that monitors the rotational speed of the engine, and the thrust power measurement line that records the thrust output of the engine for performance evaluation. The exhaust gases emitted from the engine are shown as orange arrows on the left side, flowing into the emission device for analysis. The cyan square at the bottom-right represents the fuel pump, which ensures a steady and controlled flow of fuel through the fuel line to the engine. The gray background and lines illustrate the test bench and auxiliary connections, providing structural support and indicating non-critical pathways that facilitate the overall functionality of the system. This detailed schematic layout provides a clear understanding of the experimental setup and the interactions between its components, ensuring clarity in the operation and data collection process during the performance and emission testing of the jet engine.

The experimental setup was meticulously designed to capture real-time data across a range of operating conditions, enabling a detailed analysis of the engine's performance and emissions behavior. A high-precision fuel flow meter was integrated into the setup to measure the mass flow rates of different fuel mixtures, including Jet A1, Jet A1+100 ppm TiO_2, and Jet A1+200 ppm TiO_2. The fuel consumption data were further verified using a Radwag WTC 2000 Digital Precision Scale, which has a measurement accuracy of ±0.01 g. This measurement was crucial for calculating specific fuel consumption (SFC) and assessing the impact of TiO_2 additives on fuel efficiency. Turbojet engine was mounted on a thrust stand equipped with load cells, which measured the static thrust generated at each engine speed setting. This configuration allowed for the evaluation of engine performance by correlating thrust output with fuel consumption. To monitor the exhaust gas temperature (EGT), K-type thermocouples with ±1 % measurement accuracy were placed in the exhaust stream. The thermocouples were connected to a 20-channel Graphtec Multifunctional Recorder, ensuring precise real-time temperature data collection. To further analyze the thermal efficiency and combustion quality, additional K-type thermocouples were strategically placed within the combustion chamber to monitor local gas temperatures, providing critical data for exergy analysis and understanding the influence of TiO_2 nanoparticles on temperature distribution. A Uni-T UTI165B Thermal Imaging Camera, with a temperature measurement capability of ±2° C, was used for surface temperature mapping and assessing thermal behavior in critical areas of the setup. Additionally, a CEM DT-1880 Anemometer with telescopic probes was employed to measure air velocity (0.1–20 m/s, with ±5 % +0.03 m/s accuracy) and air temperature, further contributing to the analysis of combustion dynamics. Ambient temperature and humidity were monitored using a Tfa 30.5047.54 'Exacto' Calibration-enabled Device, with an accuracy of ±1° C for temperature and ±3 % RH (35–75 %) for humidity, ensuring stable testing conditions throughout the experiments. For emission analysis, a BOSCH BEA 060 Emission Measurement Device was connected to the exhaust outlet. This device continuously measured the concentrations of key pollutants, including hydrocarbons (HC), carbon monoxide (CO), and carbon dioxide (CO_2). The analyzer provided real-time data, enabling a comprehensive assessment of the environmental impact of using TiO_2-enhanced fuels at various turbojet engine speeds.

This combination of advanced measurement systems ensured precise and reliable data collection. The setup facilitated a thorough evaluation of the effects of TiO_2 additives on both engine performance and environmental impact, providing insights into their potential for improving fuel efficiency and reducing emissions in aviation applications. The technical specifications of the emission measurement device can be seen in Table 4.

Each of these measurement systems was carefully calibrated before the experiments to ensure accuracy and reliability. The accuracy of the measurement tools and the total uncertainties calculated are given in Table 5.

Table 1
Physical Properties of the TiO_2 Nanoparticles Used in the Study [43].

Property	Specification
Product Type	Commercial TiO_2 Nanoparticles
Purity (%)	99.8
Primary Particle Size (n m)	20
Specific Surface Area (m^2/g)	35–65
Density (g/cm^3)	4.5

Table 2
The physical properties of the prepared fuels.

Fuel Properties	**Jet A1**	**Jet A1 + 100 ppm TiO_2**	**Jet A1 + 200 ppm TiO_2**
Kinematics viscosity (m m^2/ s), at 20°C	3.87	3.89	3.92
Density (g/cm^3) at 15 °C	0.775	0.781	0.789
Lower heating value (k J/kg)	42677	42497	42438
Flash point (°C)	38	38	37
Cetane number	125	126	127

Table 3
JetCat P80-SE type turbojet engine technical specification.

Parameters	Value	Unit
Dimensions (DxL),	112 × 290	m m
Weight	1360	g
Compressor pressure ratio	2.4	–
Maximum thrust,	97	N
Maximum speed	125,000	RPM
Fuel consumption (at maximum speed),	0.272	k g.m in − 1
Exhaust gas temperature (at maximum speed)	973	K

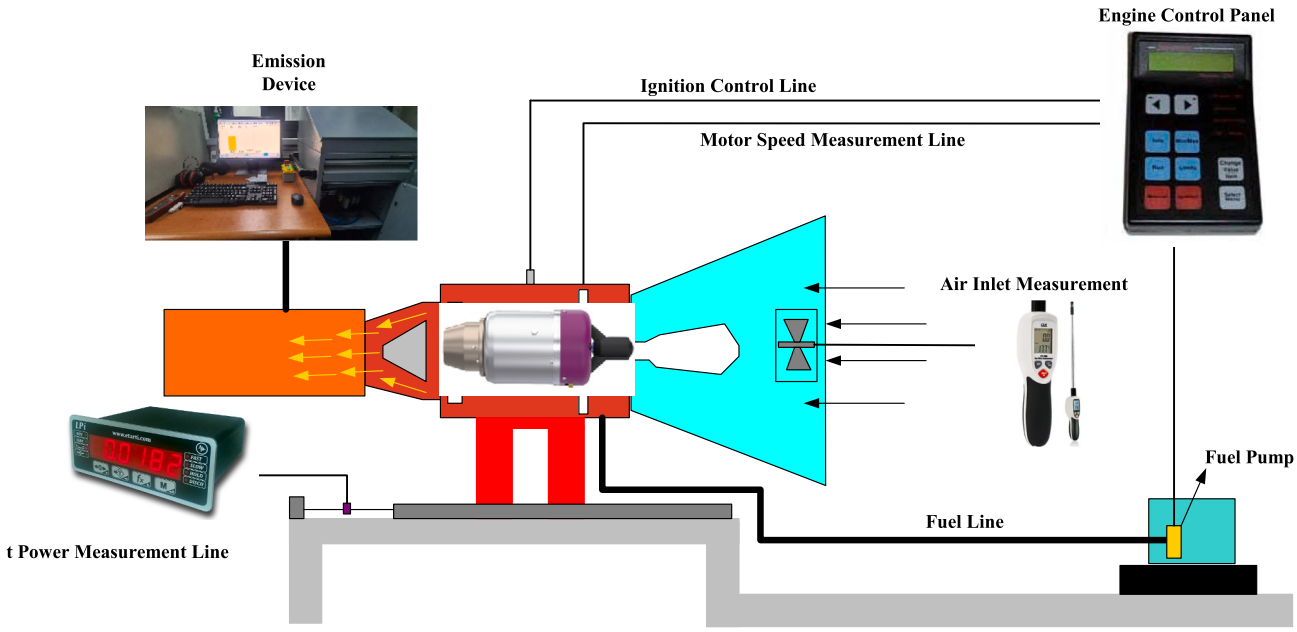

Fig. 1. Schematic representation of experimental test setup.

Table 4
Exhaust emissions device's technical properties.

Measurement	Measuring Range	Resolution	Precision
CO (vol%)	0–10	0.01	± 1 %
CO_2 (vol%)	0–18	0.01	± 0.2 %
HC (p pm)	0–9.999	1	± 1
O_2 (vol%)	0–22	0.1	± 0.1 %
NO_x (p pm)	0–5000	1	± 1
Smoke opacity (%)	0–20	0.01	± 2

Table 5
Measurement Tools Accuracy and Total Uncertainties.

Measurement	Resolution	Precision
Specific Fuel Consumption (g/s)	0.1	± 1.5 %
Static Thrust (N)	0.01	± 1 %
Exhaust Gas Temperature (^oC)	±1	± 1 %
Mass air flow rate (k g/s)	0.03	± 5 %

The data collected from the test setup were recorded and analyzed to draw conclusions about the performance improvements and emissions reductions associated with the use of TiO_2 nanoparticles in Jet A1 fuel. The tests were performed at nine different engine speeds to evaluate the effects of TiO_2 nanoparticles across a range of operational conditions. The engine speeds tested were 40 k, 50 k, 60 k, 70 k, 80 k, 90 k, 100 k, 110 k, and 120 k rpm.

3. Theoretical calculations

A small UAV jet engine consists of subsystems including a compressor, combustion chamber, and turbine. In other words, the jet engine comprises a turbine, which also forms the aircraft's propulsion system, a radial compressor directly connected to the turbine, and a circular combustion chamber. As depicted in Fig. 2, points 1–2 represent the compressor in the jet engine module, points 2–3 denote the combustion chamber, and points 3–4 symbolize the gas turbine.

In this system, the fuel supply system includes a fuel tank, fuel pump, slide valve, and electronic control card, whereas the ignition system consists of an auxiliary fuel valve, igniter plug, and starter motor. The jet

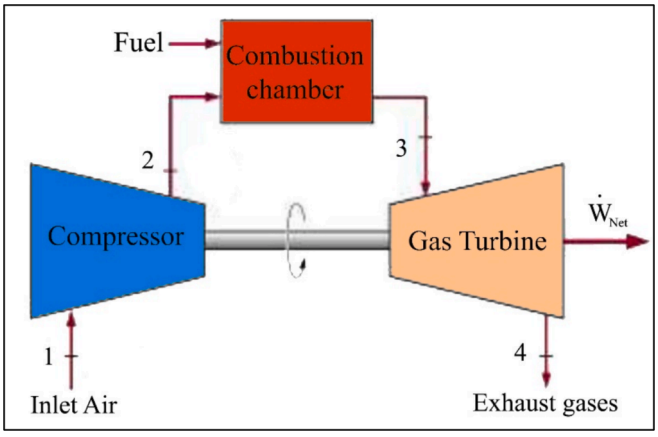

Fig. 2. Schematic view of jet engine system components [44].

engine system operates generally as follows:

High-temperature and high-pressure air from the compressor passes through the combustion chamber and is directed to the flame tube. For the combustion process to occur, the liquid fuel to be used is sent to the vaporization tubes to evaporate and convert into gas. In this section, the vaporized and gaseous fuel mixes with air in the combustion chamber. The burned gases pass through the turbine, and the exhaust gas jet increases its speed as it passes through the nozzle.

The system in Fig. 1 operates according to the open cycle principle, where air is taken from the surrounding environment, undergoes combustion, and the resulting exhaust products are expelled back into the environment. In this cycle, the air used passes through the following processes until it becomes exhaust gas [45]:

1. The ambient air is taken into the system at temperature T_1 and pressure P_1 undergoes adiabatic compression in the compressor, resulting in air temperatures and pressures of T_2 and P_2, respectively.
2. Inside the combustion chamber, the gaseous fuel reacts with oxygen, leading to combustion and isobaric heat input, raising the air temperature from T_2 to T_3.

3. The burned gases expand within the turbine, and the pressure drops rapidly to match ambient pressure. The decrease in pressure and heat losses cause the temperature to drop from T_3 to T_4.
4. As the burned gases expand in the turbine and are expelled into the surrounding environment, the mechanical work obtained during this process drives the compressor via the shaft.

To simplify energy and exergy analyses in the jet engine, some assumptions are made: The jet engine is assumed to be in a steady state, combustion is assumed to be complete, and the air and combustion gases are assumed to be ideal gases. Changes in kinetic and potential energy are neglected. The ambient air pressure is taken as 101 kPa, and the ambient air temperature is taken as 291 K in the calculations.

3.1. Energy analysis

Separate energy and exergy evaluations of the jet engine's compressor, combustion chamber, and gas turbine components are conducted based on the open gas turbine cycle. In ideal engine cycles, it is assumed that no irreversibilities occur throughout the process, whereas in real engine cycles, factors such as heat loss, friction loss, and other irreversibilities are known to affect performance.

In Eq. (1), the energy balance for the control volume of the jet engine can be obtained using the first law of thermodynamics [46,47]:

$$\dot{Q} - \dot{W} + \sum \dot{E}n_{in} - \sum \dot{E}n_{out} = 0 \tag{1}$$

Here $\dot{Q}$, $\dot{W}$ and $\dot{E}$ symbolize heat, work, and energy rates, respectively.

To apply energy and exergy analyses in a gas turbine jet engine, the enthalpy, heat energy, and work ratios of the compressor, combustion chamber, and gas turbine are calculated, respectively. Considering the control volume is in a steady state, the mass entering the system is assumed to be equal to the mass exiting the system (Eq. 2). Here, $\dot{m}_1$ and $\dot{m}_2$ represent the mass flow rate entering the system and the mass flow rate exiting the compressor, respectively, while $\dot{m}_a$ represents the mass flow rate of air.

$$\dot{m}_1 = \dot{m}_2 = \dot{m}_{air} \tag{2}$$

Additionally, in Eq. (3), the compressibility fraction (cf) is obtained by dividing the pressure of the air exiting the compressor (P_2) by the ambient pressure (P_1).

$$cf = P_2/P_1 \tag{3}$$

The work done by the compressor ($\dot{W}_{Comp}$) at adiabatic conditions can be calculated with Eq. (4).

$$\dot{W}_{Comp} = \dot{m}_{air}\left(c_{p,2}T_2 - c_{p,1}T_1\right) \tag{4}$$

In the combustion chamber component of the jet engine, the fuel energy ($\dot{E}n_f$) is obtained by multiplying the fuel mass flow rate ($\dot{m}_f$) by the lower heating value of the fuel (Q_f), as seen in Eq. (5). At this stage, as seen in Eq. (6), the fuel mass flow rate ($\dot{m}_{fuel}$) is added to the $\dot{m}_{air}$, thereby obtaining the total gas flow rate ($\dot{m}_{gas}$). The gas index in $\dot{m}_{gas}$ can be defined as combustion products.

$$\dot{E}n_f = \dot{m}_{fuel}Q_f \tag{5}$$

$$\dot{m}_{air} + \dot{m}_{fuel} = \dot{m}_{gas} \tag{6}$$

As seen in Eq. (7), the mass flow rate entering and exiting the gas turbine is equal to the mass flow rate of the combustion product gases.

$$\dot{m}_3 = \dot{m}_4 = \dot{m}_{gas} \tag{7}$$

The work done by the gas turbine ($\dot{W}_{GT}$) can be calculated with Eq. (8). Unlike the compressor, it is considered that there is heat loss to the surroundings during the operation of the gas turbine, and therefore it is not adiabatic. Due to significant heat loss during combustion, the work ratio of the gas turbine is assumed to be equal to the work ratio of the compressor. Also, Yucer [45] stated that significant heat loss occurs in the gas turbine and that the work of the gas turbine is equal to the work of the compressor.

$$\dot{W}_{GT} = \dot{m}_{gas}\left(c_{p,3}T_3 - c_{p,4}T_4\right) - Q_{loss} \tag{8}$$

The specific heat capacities of air ($c_{p,air} = c_{p,1} = c_{p,2}$) and combustion gases ($c_{p,gas} = c_{p,3} = c_{p,4}$) can be found with Eq. (9) and Eq. (10) [48].

$$c_{p,air}(T) = 1.04841 + 3.83x10^{-4}T + 9.45x10^{-7}T^2 - 5.49x10^{-10}T^3 + 7.92x10^{-14}T^4 \tag{9}$$

$$c_{p,gas}(T) = 0.9874 + 5.44x10^{-5}T + 1.48x10^{-7}T^2 - 1.48x10^{-11}T^3 \tag{10}$$

3.2. Exergy analysis

In Eq. (11), the energy balance for the control volume of the jet engine under stable state can be obtained using the second law of thermodynamics [49,50]:

$$\dot{Q} - \dot{W} + \sum \dot{E}x_{in} - \sum \dot{E}x_{out} - \sum \dot{E}x_{Dest.} = 0 \tag{11}$$

The total conversion of a flow's enthalpy into work within a system is not possible due to irreversibilities, which arise from various factors such as friction, unbalanced expansion, mixing of two flows, heat transfer, and combustion reactions. The physical exergy of a flow can be found using Eq. (12) [51]. Here, h represents the enthalpy of the component at state i, while s symbolizes the entropy at state i.

$$\dot{E}x_{ph,i} = \dot{m}_i[(h_i - h_0) - T_0(s_i - s_0)] \tag{12}$$

$$h_i - h_0 = c_{p,i}(T_i - T_0) \tag{13}$$

$$s_i - s_0 = c_{p,i}\ln\frac{T_i}{T_0} + R\ln\frac{P_i}{P_0} \tag{14}$$

If the enthalpy and entropy differences in Eq. (12) are substituted by Eq. (13) and (14) respectively, Eq. (15) is obtained. Here, $c_{p,i}$ and R represent the specific heat at constant pressure and the universal gas constant, respectively, while T_i and P_i represent the temperature and pressure at state i, respectively.

$$\dot{E}x_{ph,i} = \dot{m}_i\left[c_{p,i}(T_i - T_0) - T_0\left(c_{p,i}\ln\frac{T_i}{T_0} + R\ln\frac{P_i}{P_0}\right)\right] \tag{15}$$

E q. (16) is applied to the compressor, combustion chamber, and gas turbine components of the jet engine, respectively. Here, $\dot{E}x_{in,i}$, $\dot{E}x_{out,i}$, and $\dot{E}x_{Dest,i}$ represent the exergy entering the system, the exergy exiting the system, and the exergy destruction at state i, respectively.

$$\dot{E}x_{in,i} = \dot{E}x_{out,i} + \dot{E}x_{Dest,i} \tag{16}$$

Exergy flow formulas for the compressor component can be calculated with Eq. (17) and Eq. (18). The reason for state 1 being equal to zero in Eq. (17) is due to the lack of work potential of the compressor under ambient conditions.

$$\dot{E}x_1 = 0 \tag{17}$$

$$\dot{E}x_1 + \dot{W}_{Comp} = \dot{E}x_2 + \dot{E}x_{D,C} \tag{18}$$

In Eq. (18), $\dot{E}x_1$, $\dot{W}_{Comp}$, $\dot{E}x_2$, and $\dot{E}x_{D,C}$ represent the physical exergy at state 1, compressor work, physical exergy at state 2, and compressor exergy destruction, respectively.

Exergy destruction for the compressor can be calculated with Eq.

(19).

$$\dot{E}x_{D,C} = \dot{E}x_1 + \dot{W}_{Comp} - \dot{E}x_2 \quad (19)$$

Exergy flow formula for the combustion chamber component can be calculated with Eq. (20). Here, $\dot{E}x_{fuel}$, $\dot{E}x_3$, and $\dot{E}x_{D,CC}$ symbolize fuel exergy, physical exergy in state 3, and exergy destruction of the combustion chamber component, respectively.

$$\dot{E}x_2 + \dot{E}x_{fuel} = \dot{E}x_3 + \dot{E}x_{D,CC} \quad (20)$$

Fuel exergy can be obtained by multiplying the $\dot{m}_{fuel}$, fuel lower heating value ($\dot{Q}_{fuel}$), and chemical exergy factor (φ), as seen in Eq. (21). The chemical exergy factor for liquid fuels obtained by Kotas [52] can be determined by substituting the H/C ratio, O/C ratio, and S/C ratio from the chemical formula of the fuel into Eq. (22).

$$\dot{E}x_{fuel} = \dot{m}_{fuel}\dot{Q}_{fuel}\varphi_{fuel} \quad (21)$$

$$\varphi_{fuel} = 1.0401 + 0.1728(H/C) + 0.0432(O/C) + 0.2169(S/C)\left(1 - \frac{2.0628H}{C}\right) \quad (22)$$

Exergy destruction for the combustion chamber can be calculated with Eq. (23).

$$\dot{E}x_{D,CC} = \dot{E}x_2 + \dot{E}x_{fuel} - \dot{E}x_3 \quad (23)$$

The exergy flow and exergy destruction ($\dot{E}x_{D,GT}$) of the gas turbine (GT) component can be calculated by Eq. (24) and Eq. (25), respectively.

$$\dot{E}x_3 = \dot{E}x_4 + \dot{W}_{GT} + \dot{E}x_{D,GT} \quad (24)$$

$$\dot{E}x_{D,GT} = \dot{E}x_3 - (\dot{E}x_4 + \dot{W}_{GT}) \quad (25)$$

The exergy efficiencies of the compressor, combustion chamber and gas turbine components in the jet engine can be calculated with Eq. (26) [53]. Here, it is obtained by dividing the exergy rates entering the jet engine component by the exergy rates leaving the component.

$$\psi_k = \frac{\dot{E}x_{out,k}}{\dot{E}x_{in,k}} = 1 - \frac{\dot{E}x_{D,k}}{\dot{E}x_{in,k}} \quad (26)$$

3.3. Environmental impact analysis

Environmental, social, and economic impacts of different TiO_2 nanoparticle additives on a jet engine running on kerosene (Jet A1) fuel are examined. The environmental impact (Env_{im}) parameter is used to indicate the environmental impact of emissions obtained from experiments conducted with different engine speeds and test fuels. Env_{im} can be calculated using Eq. (20) [54]. Here, $\dot{m}_{e,i}$ and e_i represent the mass flow rate of the exhaust gases and the specific environmental impact coefficient, respectively. As seen in Table 1, e_i varies for each emission parameter.

$$Env_{im,i} = \dot{m}_{e,i}.env_i \quad (20)$$

The enviro-economic ($Env_{eco,i}$) analysis can be calculated using Eq. (21) [54]. Here, the environmental-economic impact of exhaust emissions released into the environment as a result of different TiO_2 nanoparticle additives in a jet engine running on kerosene fuel is examined. The specific environmental-economic coefficient (eco_i) for each emission is expressed in Euros per unit mass and varies in comparison to each other.

$$Env_{eco,i} = \dot{m}_{e,i}.eco_i \quad (21)$$

Similarly, the environmental-social cost impact ($Env_{sc,i}$) can be calculated using Eq. (22) [55]. The environmental-social cost impacts of using the test fuels are obtained by multiplying each exhaust component by its specific environmental-social cost coefficient (esc_i).

$$Env_{sc,i} = \dot{m}_{e,i}.esc_i \quad (22)$$

Table 6 presents the *e*, *eco* and *esc* values of each exhaust component. For the calculation of environmental and economic impacts, the HC emissions released into the environment after combustion are assumed to be CH_4. Additionally, the average exchange rate of the Euro for the year 2023 (1 $ = 0.924 €) has been taken into account.

4. Results and discussion

4.1. Performance and emissions

Fig. 3 shows the variations of SFC for Jet A1, Jet A1+100 ppm TiO_2, and Jet A1+200 ppm TiO_2 fuels at varying engine speeds. As the engine speed changes from 40 k to 120 k engine speed, the SFC values for all test fuels tend to decrease. Additionally, adding TiO2 nanoparticles to Jet A1 fuel plays a significant role in reducing SFC. TiO_2 improves the properties of the fuel, such as viscosity and lower heating value, which contributes significantly to the reduction of SFC. Furthermore, the increase in the surface-to-volume ratio in the combustion zone due to TiO_2 also enhances the combustion process. In addition, the use of nanoparticles in the fuel increases the thermal conductivity during combustion, causing the flame temperature to increase. All these reasons contribute to more efficient fuel combustion and reduced fuel consumption. Örs and others [37] report that using TiO_2 nanoparticles improves the combustion process, leading to reduced fuel consumption. The highest reduction in SFC values occurs at 60 k engine speed with the Jet A1+200 ppm TiO_2 fuel at a rate of 23 %. When using Jet A1+200 ppm TiO_2 fuel in the jet engine, SFC values decrease by 18–23 % in the 40 k to 80 k rpm range and 7–14 % in the 90 k to 120 k rpm range. On the other hand, with Jet A1+100 ppm TiO_2 fuel, SFC values decrease by 2–15 % in the 40 k to 80 k rpm and by 4–9 % in the 90 k to 120 k rpm range. The average reduction in SFC for Jet A1+100 ppm TiO_2 and Jet A1+200 ppm TiO_2 fuels compared to Jet A1 fuel is 9 % and 16 %, respectively, across the tested speed ranges. The decreased SFC with the use of TiO_2 in the current study is consistent with the results of the study by Wang et al. [59].

In summary, using TiO_2 in Jet A1 fuel reduces fuel consumption and achieves current thrust with less energy. Commercially, this implies that by incorporating TiO_2 nanoparticles into the high-cost Jet A1 fuel used in the aviation sector, lower fuel consumption can be achieved, potentially reducing operational costs.

Fig. 4 shows the variations of exhaust gas temperature (EGT) for Jet A1, Jet A1+100 ppm TiO_2, and Jet A1+200 ppm TiO_2 fuels at varying engine speeds. As the engine speed increases, the amount of fuel consumed also increases, which in turn increases the amount of energy released. Higher energy content leads to higher combustion temperatures and consequently higher EGT. Also, the gradual addition of TiO_2 to Jet A1 fuel causes an increase in EGT. Due to the thermal conductivity of TiO_2 and the increase in the combustion surface area in the combustion zone, the combustion temperature increases. This can be seen as the main reasons for the increase in EGT. When examining the three test fuels, it is observed that their EGT values are quite close to each other. The highest increase in EGT values occurs at 80 k engine speed with the

Table 6
Specific environmental impact, environmental-economic cost and environmental-social costs for each emission measurement [54,56–58].

Emissions	env_i (mPts/kg)x10^3	eco_i (Euro/kg)	esc_i (Euro/kg)
HC	0.115	3.749	7.642
CO	8.36x10^{-3}	0.278	3.844
CO_2	5.45x10^{-3}	0.123	0.065
NO_x	2.749	6.739	22.917

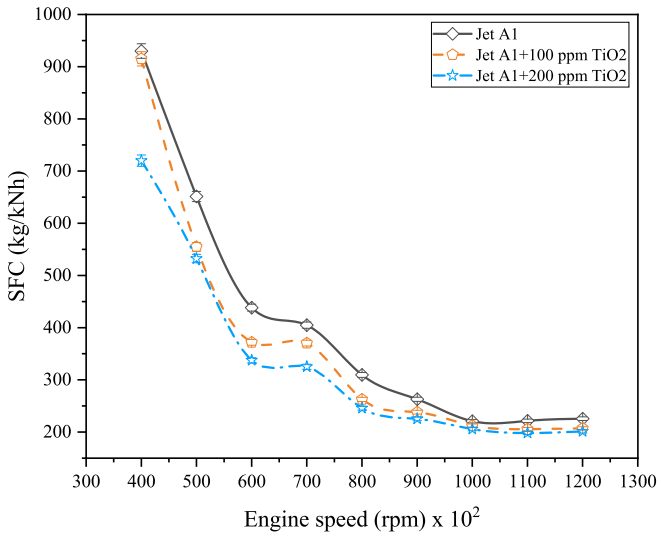

Fig. 3. Variation of SFC of jet engine at different engine speeds and test fuels.

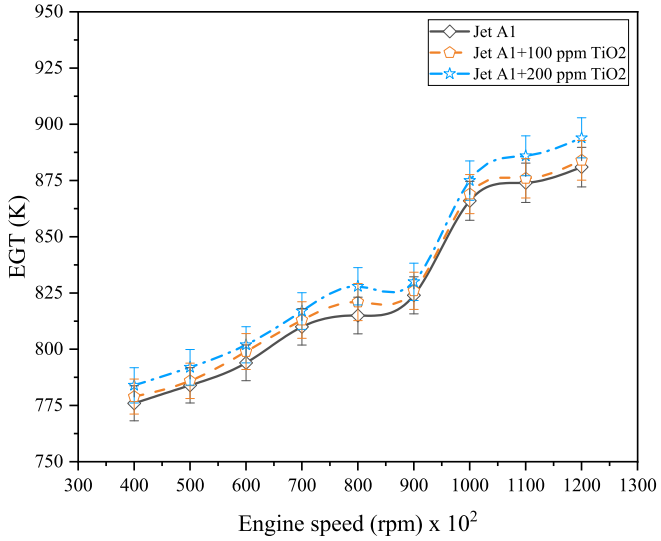

Fig. 4. Variation of EGT of jet engine at different engine speeds and test fuels.

Jet A1+200 ppm TiO_2 fuel at a rate of 1.6 %. On the other hand, the average increase in EGT for Jet A1+200 ppm TiO_2 fuel compared to Jet A1 fuel is 1 %. Jet A1+100 ppm TiO_2 fuel does not show a significant change in EGT compared to Jet A1.

Fig. 5(a) shows the variations of static thrust for Jet A1, Jet A1+100 ppm TiO_2, and Jet A1+200 ppm TiO_2 fuels at varying engine speeds. The lowest thrust force is obtained as 4 Nm with Jet A1 and Jet A1 + 100 ppm TiO_2 fuels at 40 k rpm. The highest thrust force is achieved as 56 N with Jet A1+200 ppm TiO_2 fuel at 120 k rpm. Overall, it is observed that the addition of TiO_2 nanoparticles contributes to the increase in static thrust force. This can be attributed to the fact that TiO_2 improves fuel properties (increase in thermal conductivity and energy density) and increases combustion efficiency. When considering the percentage increases in thrust, the highest increase of 25 % occurs with Jet A1+200 ppm TiO_2 (at 40 k rpm). Across the shaft speed range from 40 k to 120 k rpm, the average increase in thrust compared to Jet A1 fuel is 14.5 %. Jet A1+100 ppm TiO_2 fuel shows an average increase in thrust of 8 % compared to Jet A1.

Fig. 5(b) shows the variations of air mass flow rate for Jet engine at varying engine speeds. In this study, all exergy and environmental calculations assume that the ambient temperature and pressure remain constant to simplify the analysis. Therefore, it can be assumed that the density of the intake air and the surface area of the intake channel do not change, and minimal changes in intake air velocity do not affect the mass flow rate. In this case, the liquid fuels used in the tests are considered to have a negligible effect on the intake air flow rate. Indeed, Gürbüz and colleagues [54] emphasized that the addition of hydrogen minimally affects the intake air in a Euro diesel-hydrogen dual-fuel turbojet engine and that this effect is negligible. Consequently, the air mass flow rates indicated in the figure are used for all test fuels in this study. The lowest air mass flow rate is 0.105 kg/s at 40 k rpm, while the highest air mass flow rate is 0.302 kg/s at 120 k rpm.

Fig. 6 shows the variation of HC, NO_x, CO, and CO_2 emissions for Jet A1, Jet A1+100 ppm TiO_2, and Jet A1+200 ppm TiO_2 fuels at varying engine speeds. HC emissions can occur due to fuel accumulation in blind spots where the flame front cannot progress, as well as incomplete combustion resulting from the physical properties of the fuel and operating parameters. This situation is directly related to the combustion process[60]. As the engine speed changes from 40 k to 120 k rpm, HC emissions show a decreasing trend for all test fuels. HC emissions tend to decrease with higher in-cylinder combustion temperatures and increased intake air concentration. Therefore, in this study, as the engine speed increases, the intake air flow rate also increases, and the combustion temperatures rise due to a more advanced combustion phase. This contributes to the reduction of HC emissions. The lowest HC emissions are obtained with Jet A1+200 ppm TiO_2 fuel at 120 k rpm, while the highest HC emissions are observed with Jet A1 fuel at 40 k

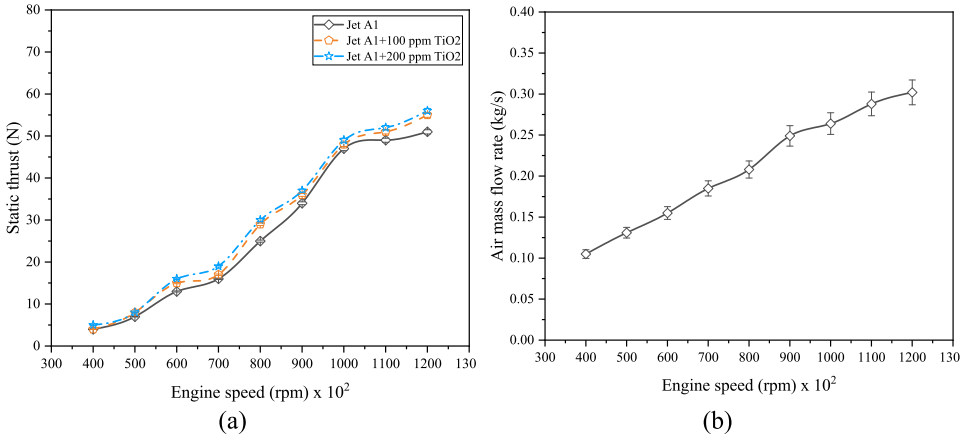

Fig. 5. Variation of (a) static thrust and (b) air mass flow rate of jet engine at different engine speeds and test fuels.

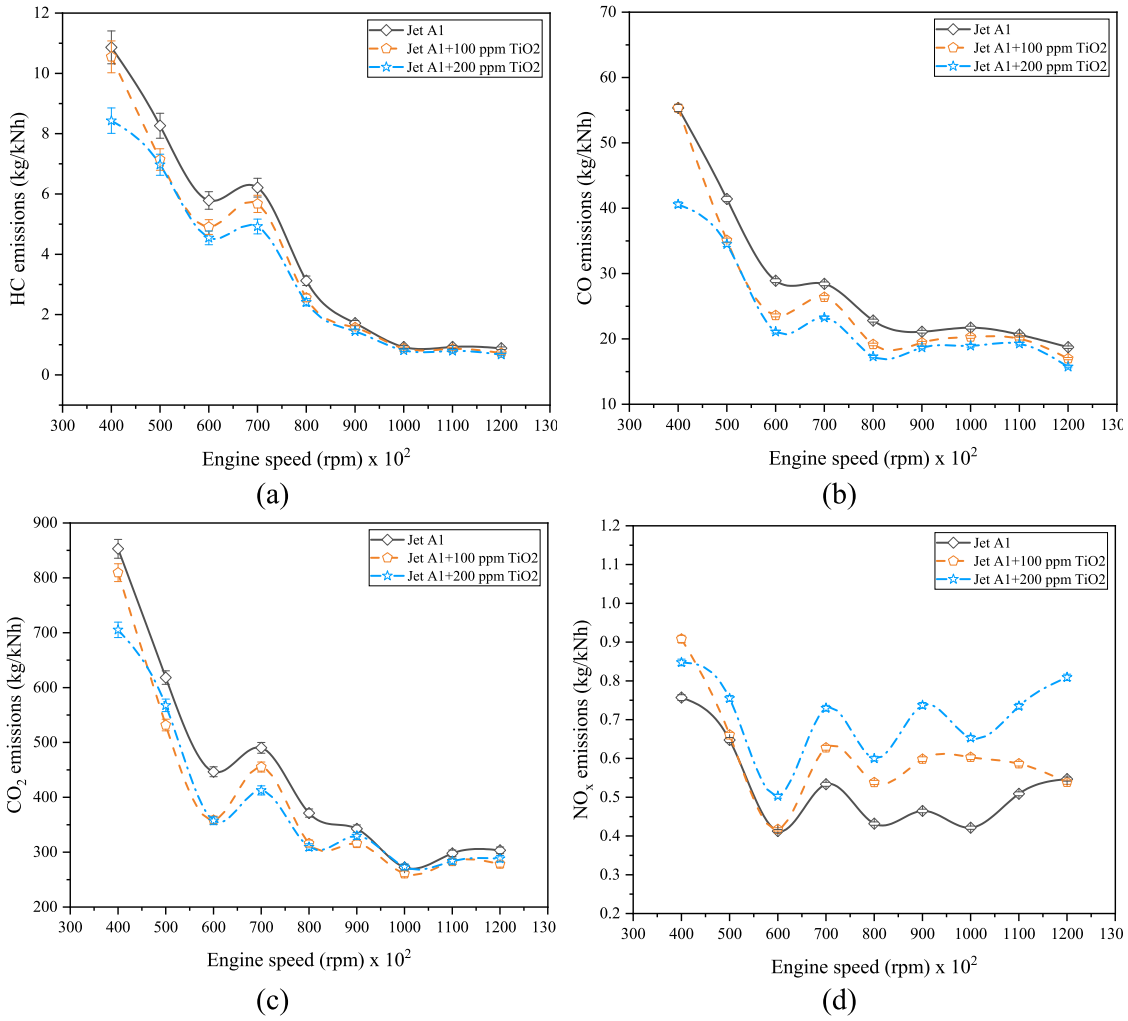

Fig. 6. Variation of (a) HC, (b) CO, (c) CO_2, and (d) NO_x emissions of jet engine at different engine speeds and test fuels.

rpm. From Fig. 6(a), adding TiO_2 nanoparticles contributes to reducing HC emissions. The primary reasons for the reduction in HC emissions are the increase in surface/volume ratio thanks to using TiO_2 in the combustion chamber and the catalytic role of TiO_2 in accelerating HC reactions. Additionally, the oxygen content of TiO_2 accelerates oxidation activity in the combustion zone, thereby increasing combustion stability and contributing to a reduction in HC emissions. Furthermore, its ability to reduce fuel consumption also promotes the use of lower carbon fuels. As a result, this leads to lower levels of HC emissions released compared to what would normally be emitted. Similar results regarding the reduction of HC emissions due to the use of TiO_2 nanoadditives can be found in the literature: D'Silva and colleagues [40] report that TiO_2 nanoadditives create an O_2 buffer within the fuel, thereby enhancing combustion and reducing HC emissions. Within the specified engine speed ranges, the average reduction in HC emissions for Jet A1+100 ppm TiO_2 and Jet A1+200 ppm TiO_2 fuels compared to Jet A1 fuel is 11 % and 19 %, respectively. Also, the HC emissions of Jet A1+200 ppm TiO_2 fuel show a decreasing trend of 15–23 % compared to Jet A1 fuel in the 40 k to 90 k rpm range. In the same rpm range, the reduction rate of HC emissions for Jet A1+100 ppm TiO_2 fuel varies between 0–18 %. Shao et al. [61] have stated that the use of TiO_2 improves the combustion phase and increases combustion efficiency, thereby potentially reducing emissions.

Fig. 6(b) shows that, similar to HC emissions, CO emissions decrease with the increase in engine speed from 40 k to 120 k rpm. Additionally, it can be seen that the use of TiO_2 nanoparticles in Jet A1 fuel results in a reduction of CO emissions. The highest rate of CO emission reduction occurs at 60 k rpm with Jet A1+200 ppm TiO_2 fuel, achieving a 27 % reduction. When using Jet A1+200 ppm TiO_2 fuel in the jet engine, CO emissions decrease by 18–27 % in the 40 k to 80 k rpm range, and by 7–16 % in the 90 k to 120 k rpm range. On the other hand, with Jet A1+100 ppm TiO_2 fuel, CO emissions decrease by 1–18 % in the 40 k to 80 k rpm range, and by 3–9 % in the 90 k to 120 k rpm range. The average reduction in CO emissions for Jet A1+100 ppm TiO_2 and Jet A1+200 ppm TiO_2 fuels compared to Jet A1 fuel is 9 % and 18 %, respectively, across the tested speed ranges. The decrease in CO emissions with increasing engine speed can be attributed to the rise in combustion temperatures. This is because CO emissions continue to convert to CO_2 at high temperatures and in the presence of high O_2 levels. Pulkrabek [62] emphasizes that high combustion temperatures and high O_2 levels reduce CO emissions.

Fig. 6(c) shows the changes in CO_2 emissions at different engine speeds and with different test fuels. Although using TiO_2 nanoparticles results in a percentage increase in CO_2 emissions, the emissions per unit kN are lower compared to Jet A1 fuel. This indicates that using TiO_2 nanoparticles contributes to reducing greenhouse gas emissions under the operational conditions (load and speed) of the jet engine. While the Jet A1+200 ppm TiO_2 fuel shows a reduction of 8–17 % in the 40 k to 80 k rpm range compared to Jet A1 fuel, it has an average reduction of 10 %. Similarly, the Jet A1+100 ppm TiO_2 fuel shows a 5–15 % reduction in the same engine speed range, with an average reduction of 9.5 %.

NO_x emissions increase with the use of TiO_2 nanoparticles. This can

be explained by the fact that TiO_2 nanoparticles increase the surface-to-volume ratio and act as a catalyst in combustion reactions. NO_x emissions form at high combustion temperatures and high O_2 concentrations [63]. From Fig. 6(d), it can be seen that the increased intake air flow with engine speed is another important factor that triggers the increase in NO_x emissions. Jafarmadar and Niaki [39] also mention in their studies that the use of TiO_2 nano additives leads to the formation of oxygen-rich zones, which in turn results in an increase in NO_x emissions. In the study, the highest NO_x emission is obtained at 90 k rpm with Jet A1+200 ppm TiO_2 fuel, showing an increase rate of 58.5 % compared to Jet A1 fuel. With Jet A1+100 ppm TiO_2, this increase rate is lower, approximately 28.6 % compared to Jet A1 (at 90 k rpm). Within the specified engine speed ranges, the average increase in NO_x emissions for Jet A1+100 ppm TiO_2 and Jet A1+200 ppm TiO_2 fuels compared to Jet A1 fuel is 17 % and 37 %, respectively. The high NO_x increase rates in high engine speed ranges for both fuels can be attributed to high combustion temperatures.

Fig. 7 shows the variation of smoke emissions for Jet A1, Jet A1+100 ppm TiO_2, and Jet A1+200 ppm TiO_2 fuels at varying engine speeds. Although smoke emissions tend to increase with the engine speed rising from 40 k to 120 k rpm, the addition of TiO_2 nanoparticles to Jet A1 fuel reduces smoke emissions. The literature reports that smoke emissions occur in excessively rich mixture regions and at high temperatures [63,64]. The increased combustion temperatures with higher engine speed may cause the oxidation of C_xH_y in regions too rich to react, leading to particle formation. The experimental findings indicate that the highest smoke emissions were obtained with Jet A1 fuel, while the lowest smoke emissions were achieved with Jet A1+200 ppm TiO_2 fuel. Compared to Jet A1 fuel, the maximum reduction in smoke emissions, about 67 %, was observed at 50 k rpm with Jet A1+200 ppm TiO_2 fuel. The improvement rates in smoke emissions compared to Jet A1 fuel were approximately 30 % and 43 % on average for Jet A1+100 ppm TiO_2 and Jet A1+200 ppm TiO_2 fuels, respectively. In the literature, it is noted that the use of metal nano additives reduces smoke emissions due to its high activation energy [65,66]. Additionally, Fayad et al.[67] emphasize in their studies that the increased reaction potential of TiO_2 contributes to reducing smoke emissions.

When evaluating the current emission results, it is observed that emissions other than NO_x can be reduced with the use of TiO_2 in Jet A1 fuel. This finding is highly significant for mitigating environmental concerns related to emissions. However, the significant increase in NO_x emissions is critical from an environmental impact perspective.

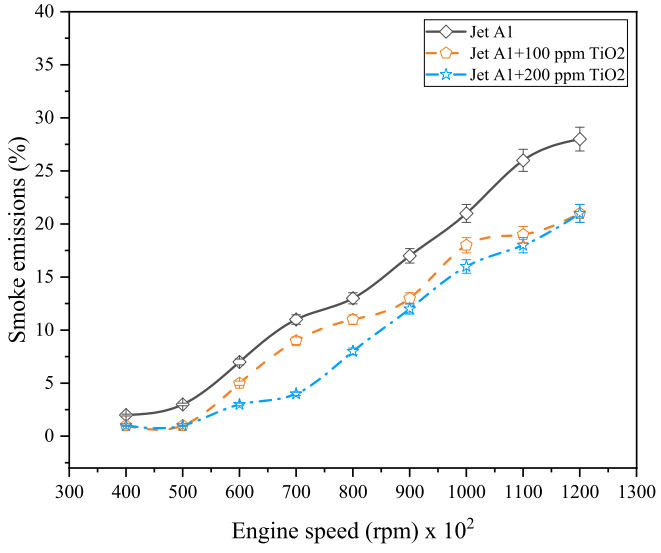

Fig. 7. Variation of smoke emissions of jet engine at different engine speeds and test fuels.

4.2. Energy and exergy analysis

In this paper, the energy and exergy analyses of a small jet engine are examined. Table 7 presents the energy flows of the jet engine, compressor work, and compressor outlet temperature. When Table 7 is analyzed, it is seen that assuming the inlet air temperature remains unchanged and the changes in air mass flow rate are neglected, the energy ratios at point 1 are the same for all test fuels. However, since the compressor output, combustion chamber temperatures and exhaust gas temperatures change at other points (2, 3 and 4), the energy flows at these points also change. The varying compressor outlet temperatures for each engine speed and test fuel cause changes in the energy flows at the compressor outlet (point 2). In this section, the highest energy rates are obtained with Jet A1+200 ppm TiO_2 fuel, while the lowest energy flows are obtained with Jet A1. The average physical energy flows at point 2 increase by 1 % and 2 % for Jet A1+100 ppm TiO_2 and Jet A1+200 ppm TiO_2 fuels compared to Jet A1, respectively. Also, at point 3, the physical energy flows increase by an average of 0.2 % and 0.3 % for Jet A1+100 ppm TiO_2 and Jet A1+200 ppm TiO_2 fuels compared to Jet A1, respectively. Increasing engine speed leads to higher fuel consumption. This results in more energy being released and, consequently, is one of the main reasons for the increase in combustion temperatures. One of the primary reasons for the increase in physical energy at point 3 is the rise in combustion temperatures. Another reason is the increase in the consumed air flow rate. As seen in Fig. 3, the addition of TiO_2 nanoadditives to Jet A1 fuel increases EGT temperatures. This contributes to the increase in physical energy flows at point 4 (gas turbine outlet). Therefore, the highest energy flows at point 4 are obtained with Jet A1+200 ppm TiO_2 fuel, followed by Jet A1+100 ppm TiO_2 fuel and Jet A1 fuel.

For all test fuels and operating conditions, the fuel energy is directly related to the lower heating value of the fuel and the fuel mass flow rate. Table 5 shows that the highest fuel energy is obtained with Jet A1, while the lowest fuel energy is obtained with Jet A1+200 ppm TiO_2 fuel. The main reason for this is the addition of TiO_2 nanoparticles to Jet A1 fuel. The addition of TiO_2 nanoparticles contributes to an increase in the lower heating value of Jet A1 fuel. It also acts as a catalyst in chemical reactions, contributing to better combustion performance due to the increased surface/volume ratio. This results in lower fuel consumption and, consequently, lower fuel energy. The fuel energy flows of Jet A1+100 ppm TiO_2 and Jet A1+200 ppm TiO_2 fuels decrease by an average of 2.5 % and 5.1 %, respectively, compared to Jet A1.

The compressor work is directly affected by the mass flow rate of air entering the compressor and the difference between the compressor outlet and inlet temperatures. Increased compressor outlet temperatures and the increased mass flow rate of air entering the system with higher engine speeds cause an increase in compressor work. The highest compressor work at all engine speeds is obtained with Jet A1+200 ppm TiO_2 fuel, while the lowest compressor work is obtained with Jet A1 fuel. The compressor work for Jet A1+100 ppm TiO_2 and Jet A1+200 ppm TiO_2 fuels is on average 1.9 % and 4 % higher than that for Jet A1, respectively.

Table 8 presents the exergy flows and exergy destructions of the jet engine component. When comparing the physical exergy values at points 2, 3, and 4 in Table 4 with the physical energy values in Table 3, they appear to be quite low. The main reason for this is the significant irreversibilities occurring in the jet engine system. The exergy flows at the compressor outlet are directly affected by the compressor outlet temperature, compressor outlet pressure, and mass air flow rate. The increase in compressor outlet temperatures with engine speed also leads to an increase in compressor outlet pressure. This causes the exergy flows at point 2 to increase as the engine speed changes from 40 k to 120 k rpm. Examining the exergy flows at point 2, the physical exergy increases by 2.6 % and 5.4 % for Jet A1+100 ppm TiO_2 and Jet A1+200 ppm TiO_2 fuels compared to Jet A1, respectively. Similarly, the increase in combustion temperatures at point 3 and EGT temperatures at point 4

Table 7
Energy flows, compressor work and compressor outlet temperature values of different test fuels and jet components.

Fuel type	Engine speed	$\dot{E}n_1$	$\dot{E}n_2$	$\dot{E}n_3$	$\dot{E}n_4$	$\dot{E}n_f$	$\dot{W}_{Comp}$	T_2
	(rpm)	(kW)	(kW)	(kW)	(kW)	(kW)	(kW)	(K)
Jet A1	40000	19.3	32.1	80.9	54.1	45.9	12.8	474
	50000	38.3	64.8	162.6	107.9	56.6	26.5	482
	60000	45.3	79.2	199.2	134.3	70.5	33.9	497
	70000	54.1	101.3	243.8	161.4	80.3	47.2	529
	80000	60.8	119.1	294.4	185.5	95.9	58.4	551
	90000	72.7	147.8	358.9	224.9	110.6	75.1	569
	100000	77.1	172.3	411.5	252.1	128.5	95.2	619
	110000	84.1	189.1	457.1	277.9	134.7	104.9	622
	120000	85.6	195.1	473.1	278.1	142.7	109.5	630
Jet A1+100 ppm TiO_2	40000	19.3	32.3	82.3	55.9	45.4	12.9	477
	50000	38.3	65.1	163.9	112.2	54.7	26.8	484
	60000	45.3	80.1	200.8	135.8	68.9	34.8	502
	70000	54.1	103.2	244.9	163.2	77.9	49.1	538
	80000	60.8	119.9	294.7	187.1	94.3	59.1	554
	90000	72.7	149.3	356.6	223.6	105.9	76.5	574
	100000	77.1	172.9	412.5	253.1	125.9	95.8	621
	110000	84.1	189.7	452.6	276.5	129.9	105.6	624
	120000	85.6	198.3	469.2	282.1	141.1	112.7	639
Jet A1+200 ppm TiO_2	40000	19.3	32.6	82.4	56.4	44.3	13.4	482
	50000	38.3	65.8	164.3	113.2	52.3	27.5	489
	60000	45.3	80.9	201.2	135.8	66.5	35.7	507
	70000	54.1	104.1	245.2	162.5	76.2	49.9	542
	80000	60.8	121.3	295.2	183.2	90.8	60.5	560
	90000	72.7	150.7	357.3	223.3	102.8	77.9	579
	100000	77.1	174.5	413.5	255.1	124.1	97.4	626
	110000	84.1	191.5	452.6	281.5	127.1	107.3	629
	120000	85.6	199.4	468.4	288.6	138.7	113.8	642

Table 8
Exergy flows and exergy destruction values of different test fuels and jet components.

Fuel type	Engine speed	$\dot{E}x_2$	$\dot{E}x_3$	$\dot{E}x_4$	$\dot{E}x_f$	$\dot{E}x_{DC}$	$\dot{E}x_{DCC}$	$\dot{E}x_{DGT}$
	(rpm)	(kW)	(kW)	(kW)	(kW)	(kW)	(kW)	(kW)
Jet A1	40000	3.8	30	12.6	49.1	9.0	22.8	4.6
	50000	8.9	59.5	24.1	60.5	17.6	9.9	8.9
	60000	11.8	75	32.2	75.3	22.2	12.1	8.8
	70000	17.2	93.3	35.1	85.7	30.1	9.7	10.9
	80000	24.6	116.6	44.8	102.4	33.8	10.4	13.5
	90000	34.2	141.8	50.6	118.1	40.8	10.6	16.1
	100000	45.3	171.8	60.5	137.2	49.9	10.7	16.1
	110000	51.9	191.6	65.8	143.8	52.9	4.1	20.9
	120000	55.5	199.8	62.7	152.4	54.1	8.1	27.6
Jet A1+100 ppm TiO_2	40000	3.9	30.8	13.6	48.5	9.1	21.6	4.2
	50000	9.1	60.3	26.5	58.5	17.7	7.3	7.0
	60000	12.2	76.6	32.9	73.7	22.6	9.2	8.8
	70000	18.1	93.5	34.5	83.2	31.0	78	9.8
	80000	25.0	116.7	45.6	100.7	34.1	9.1	12.0
	90000	35.0	139.9	49.7	113.1	41.5	8.2	13.7
	100000	45.8	172.4	60.9	134.5	50.1	7.9	15.6
	110000	52.4	188.0	64.8	138.8	53.2	3.1	17.7
	120000	57.2	196.8	63.6	150.6	55.5	11.1	20.4
Jet A1+200 ppm TiO_2	40000	4.1	30.8	13.8	47.3	9.3	20.6	3.6
	50000	9.5	60.0	25.9	55.8	18.0	5.3	6.6
	60000	12.6	77.0	32.9	71.0	23.1	6.6	8.3
	70000	18.6	93.0	33.3	81.4	31.4	7.0	9.7
	80000	25.7	116.8	44.4	97.0	34.8	5.9	11.8
	90000	35.8	140.4	48.2	109.8	42.2	5.1	14.2
	100000	46.6	172.9	62.1	132.5	50.8	6.2	13.3
	110000	53.3	187.7	64.7	135.8	54.0	1.4	15.6
	120000	57.8	196.2	65.8	148.1	55.9	9.8	16.5

contributes to the increase in exergy flows. However, at points 3 and 4, the varying amounts of total burned mass for different test fuels also lead to unpredictable exergy changes. At point 3, the physical exergy flows of 100 ppm TiO_2 and 200 ppm TiO_2 blended fuels increase by an average of 0.2 % and 0.3 %, respectively, compared to Jet A1, while at point 4, they increase by an average of 2.1 % and 1.6 %, respectively.

When examining compressor exergy destructions, the highest exergy destructions are obtained with Jet A1+200 ppm TiO_2 fuel, while the lowest exergy destructions are obtained with Jet A1 fuel. The primary reason for this is the higher compressor outlet temperature exhibited by Jet A1+200 ppm TiO_2 fuel, which increases the physical exergy flow at point 2. For all test fuels, the compressor exergy destruction flows of Jet A1+100 ppm TiO_2 and Jet A1+200 ppm TiO_2 fuels are on average 1.4 % and 3.1 % higher than those of Jet A1, respectively.

When examining exergy destruction for the combustion chamber, it is generally observed that Jet A1+100 ppm TiO_2 and Jet A1+200 ppm

TiO_2 fuels have lower exergy destruction flows compared to Jet A1 fuel. The lowest exergy destruction flows in the combustion chamber are obtained with the test fuel containing 200 ppm TiO_2, while the highest exergy destruction flows are obtained with Jet A1 fuel. In the engine speed range of 40 k-120 k rpm, the exergy destruction flows of Jet A1+100 ppm TiO_2 and Jet A1+200 ppm TiO_2 fuels decrease by an average of 14 % and 35 %, respectively, compared to Jet A1 fuel. Similarly, the addition of TiO_2 nanoparticles to Jet A1 fuel significantly reduces the exergy destruction flow of the gas turbine compared to Jet A1 fuel. At all speeds, the lowest gas turbine exergy destruction is obtained with Jet A1+200 ppm TiO_2 fuel, while the highest exergy destruction is obtained with Jet A1 fuel. The increased combustion efficiency due to the addition of TiO_2 nanoparticles and the resulting higher EGT temperatures lead to an increase in gas turbine physical exergy. The increase in gas turbine physical exergy flow directly affects the reduction of exergy destruction. In the engine speed range of 40 k-120 k, the exergy destruction flows of Jet A1+100 ppm TiO_2 and Jet A1+200 ppm TiO_2 fuels decrease by an average of 12 % and 19 %, respectively, compared to Jet A1 fuel.

Fig. 8 shows the changes in the exergy efficiency of the compressor for Jet A1, Jet A1+100 ppm TiO_2, and Jet A1+200 ppm TiO_2 fuels at varying engine speeds. As seen in Fig. 7, the compressor exergy efficiencies of all test fuels are quite close to each other. The main reason for this is that the compressor inlet temperature and air mass flow rate are assumed to be the same for all test fuels. Additionally, the increase in engine speed for all test fuels leads to an increase in compressor exergy efficiency. The main reasons for the increase in exergy efficiency are the increased mass flow rate of inlet air and the increased compressor air outlet temperatures with engine speed. Generally, the lowest compressor exergy efficiency is obtained with Jet A1 fuel at 40 k engine speed, with a value of 29.5 %. The highest compressor exergy efficiency is obtained with Jet A1+200 ppm TiO_2 fuel at 120 k rpm, with a value of 50.8 %. To compare the increases in compressor exergy efficiencies, the average increase in compressor exergy efficiency for Jet A1+100 ppm TiO_2 and Jet A1+200 ppm TiO_2 fuels in the engine speed range of 40 k to 120 k rpm is 1 % and 1.4 %, respectively, compared to Jet A1 fuel.

Fig. 9 shows the changes in the exergy efficiency of the combustion chamber for Jet A1, Jet A1+100 ppm TiO_2, and Jet A1+200 ppm TiO_2 fuels at varying engine speeds. As the engine speed varies from 40 k to 110 k rpm, the exergy efficiencies of the combustion chamber for all test fuels show an increase. The increase in the mass flow rate of gas and combustion temperatures with the increase in engine speed is seen as

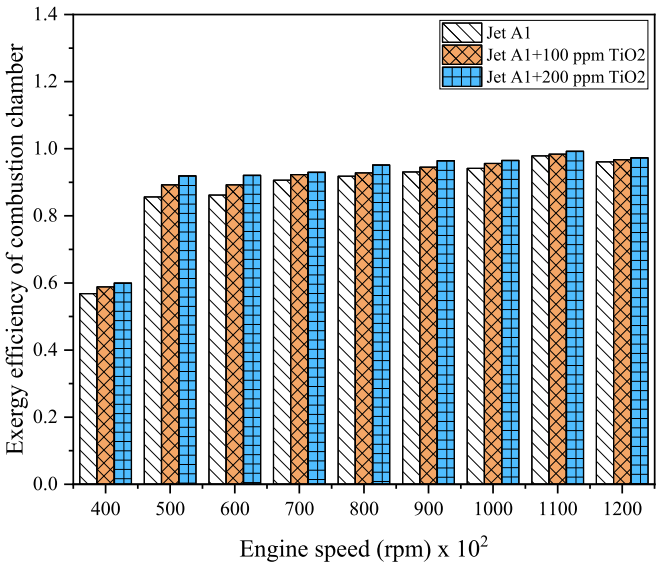

Fig. 9. Variation of exergy efficiency of combustion chamber at varying test fuels and engine speeds.

one of the reasons for this increase. Among all engine speeds, the highest combustion chamber exergy efficiency is obtained with Jet A1+200 ppm TiO_2 fuel (99.2 % at 110 k rpm), while the lowest combustion chamber exergy efficiency is obtained with Jet A1 fuel (56.8 % at 40 k rpm). The addition of TiO_2 nanoparticles increases the surface-to-volume ratio within the combustion chamber, leading to an increase in combustion efficiency and higher combustion temperatures. High combustion temperatures and lower fuel consumption are among the most significant reasons for the increase in combustion chamber exergy efficiency. In the engine speed range of 40 k to 120 k rpm, the combustion chamber exergy efficiencies of Jet A1+100 ppm TiO_2 and Jet A1+200 ppm TiO_2 fuels show an average increase of 1.8 % and 3.6 %, respectively, compared to Jet A1 fuel.

Fig. 10 shows the changes in the exergy efficiency of the gas turbine for Jet A1, Jet A1+100 ppm TiO_2, and Jet A1+200 ppm TiO_2 fuels at varying engine speeds. Unlike the exergy efficiencies of the compressor and combustion chamber, the exergy efficiencies of the gas turbine for all test fuels are obtained above 80 %. High EGT temperatures and the

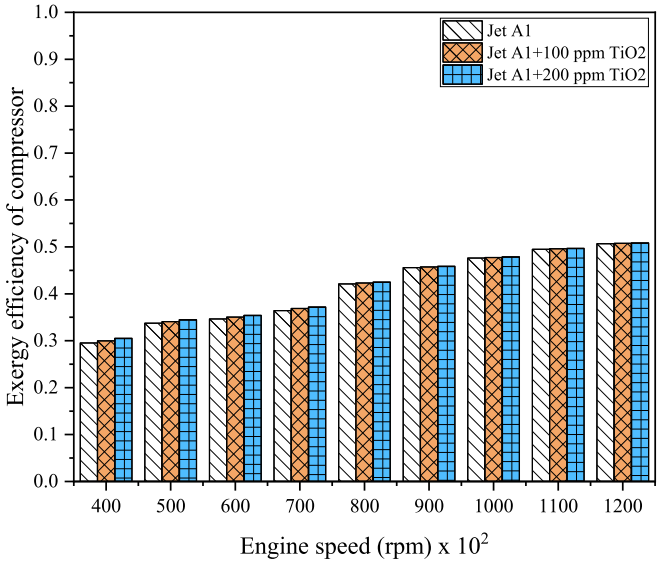

Fig. 8. Variation of exergy efficiency of the compressor at varying test fuels and engine speeds.

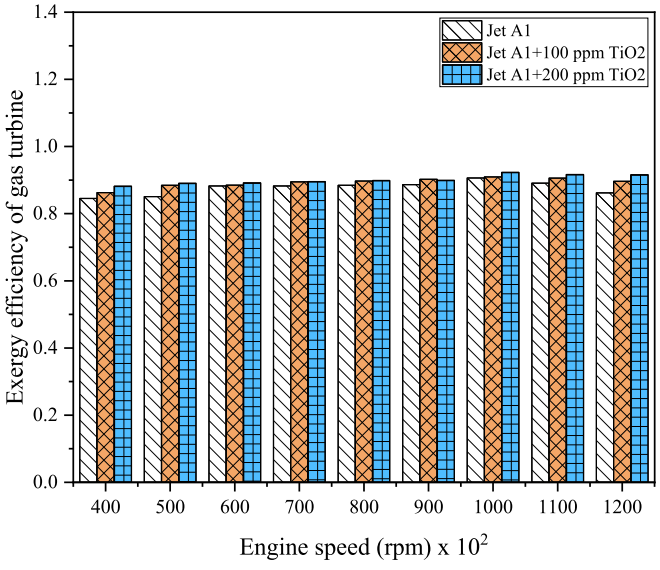

Fig. 10. Variation of exergy efficiency of gas turbine at varying test fuels and engine speeds.

increase in gas turbine work with rising engine speeds lead to a reduction in gas turbine exergy destruction and consequently an increase in gas turbine exergy efficiency. Generally, the lowest gas turbine exergy efficiency (84 % at 40 k rpm) is obtained with Jet A1 fuel, while the highest gas turbine exergy efficiency (92 % at 100 k rpm) is obtained with Jet A1+200 ppm TiO_2 fuel. The addition of TiO_2 nanoparticles to Jet A1 fuel generally contributes to the increase in gas turbine exergy efficiency. TiO_2 enhances combustion efficiency and gas temperatures, leading to higher EGT temperatures. This results in lower exergy destruction and consequently increases gas turbine exergy efficiency. In the engine speed range of 40 k to 120 k rpm, the gas turbine exergy efficiencies of Jet A1+100 ppm TiO_2 and Jet A1+200 ppm TiO_2 fuels show an average increase of 1.9 % and 2.8 %, respectively, compared to Jet A1 fuel.

When evaluating the exergy efficiencies of the compressor, combustion chamber, and gas turbine, the use of TiO_2 in Jet A1 fuel shows to be more sustainable in terms of efficiency compared to Jet A1 fuel alone. Additionally, achieving current engine speeds with less fuel and higher exergy efficiency can contribute to reducing costs from a commercial standpoint.

4.3. Enviromental impact and cost analysis

In this study, while evaluating the environmental impact and cost analysis, the mass values of the exhaust gases (g/h) emitted into the environment during one hour of operation of the turbojet engine are taken into account. Fig. 11 shows the changes in the environmental impacts of HC, NO_x, CO, and CO_2 emissions for Jet A1, Jet A1+100 ppm TiO_2, and Jet A1+200 ppm TiO_2 fuels at varying engine speeds. The environmental impact values of HC, NO_x, CO, and CO_2 are evaluated based on unit thrust (kN) to show the effect of engine speed variation. In all emissions, although the lowest specific environmental impact value (see Table 4) belongs to CO_2 emissions, CO_2 emissions still show the highest environmental impact value among these emissions. The main reason for this is the higher concentration of CO_2 emissions compared to other emissions (see Fig. 6). Additionally, adding TiO_2 nanoparticles to Jet A1 fuel contributes to reducing CO_2's environmental impact. The main reason for this is that the increase in combustion efficiency due to TiO_2 reduces fuel consumption and, consequently, the total exhaust gas concentration. The average reduction rates in CO_2 environmental impact for Jet A1+100 ppm TiO_2 and Jet A1+200 ppm TiO_2 fuels compared to Jet A1 fuel in the 40 k to 120 k rpm range are 9.5 % and 10 %, respectively. After CO_2 emissions, the other exhaust gas with the highest environmental impact is NO_x, followed by HC and CO emissions. Although the NO_x concentration in the jet engine's exhaust emissions is low, the high specific environmental impact coefficient of NO_x increases its environmental impact. Generally, the addition of TiO_2 to Jet A1 fuel, which improves combustion and increases combustion temperatures, causes an increase in NO_x, resulting in an increased environmental impact of NO_x. The average increase rates in NO_x environmental impact

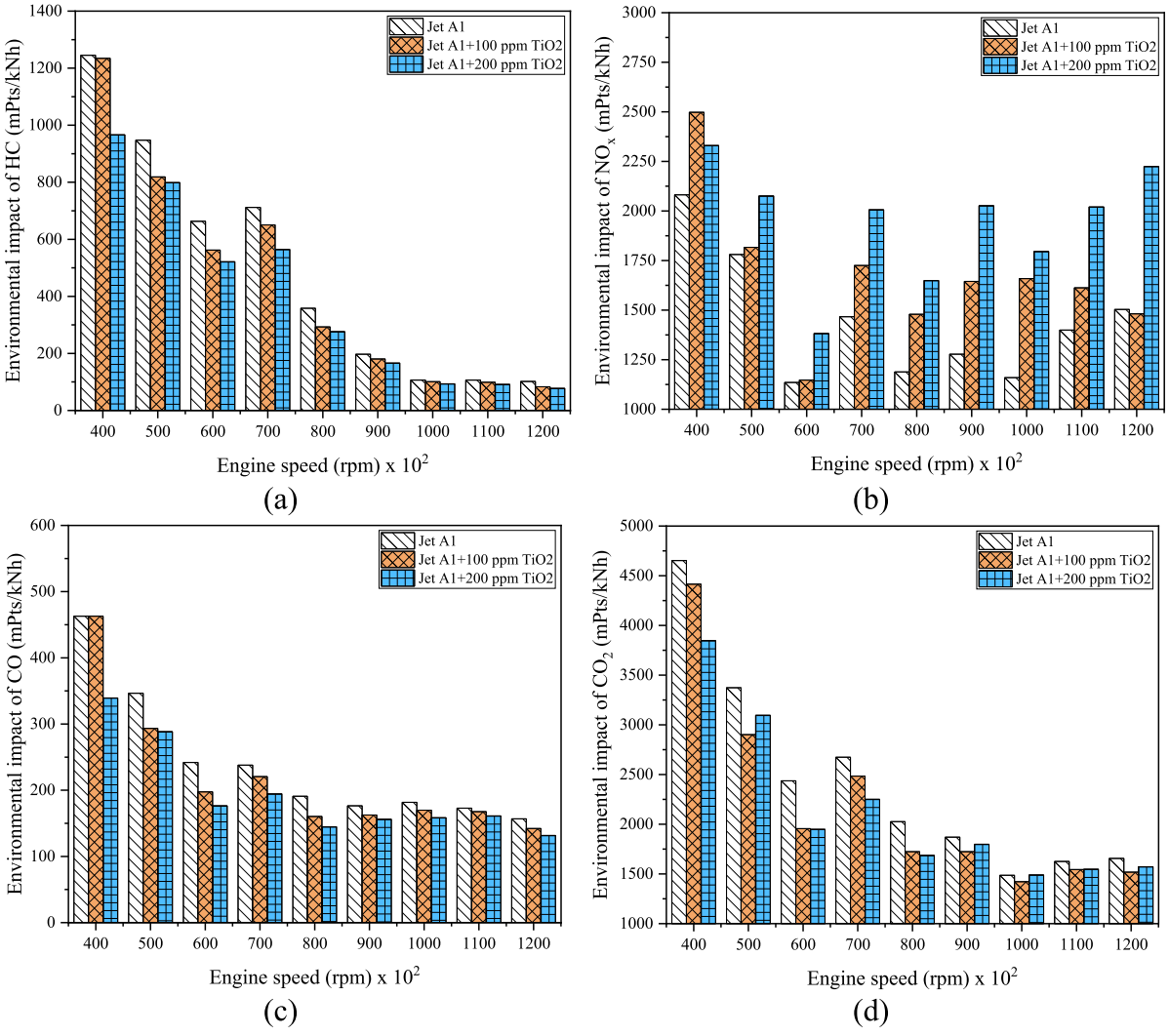

Fig. 11. Variation of environmental impact of (a)HC, (b)NO_x, (c)CO, and (d)CO_2.

for Jet A1+100 ppm TiO_2 and Jet A1+200 ppm TiO_2 fuels compared to Jet A1 fuel in the 40 k to 120 k rpm range are 17 % and 37 %, respectively.

HC emissions are the third most impactful exhaust emission compound after CO_2 and NO_x in terms of environmental impact. As seen in Fig. 11(a), adding TiO_2 nanoparticles to Jet A1 fuel contributes to reducing HC environmental impact at all engine speeds. The main reason for this is the catalytic property of TiO_2, which accelerates reactions and ensures more efficient combustion. Additionally, reducing fuel consumption with increased combustion efficiency significantly contributes to reducing HC environmental impact. The average reduction rates in HC environmental impact for Jet A1+100 ppm TiO_2 and Jet A1+200 ppm TiO_2 fuels compared to Jet A1 fuel in the 40 k to 120 k rpm range are 11 % and 19 %, respectively. Another important environmental impact compound, CO emissions, have the lowest impact among the other emissions. The increased air flow rate and decreased fuel consumption with increasing speed contribute to the reduction of carbon ratio. Moreover, the catalytic property of TiO_2 accelerates reactions, aiding in the completion of the CO to CO_2 conversion process. Additionally, the fact that CO has the second-lowest specific environmental impact coefficient after CO_2 is one of the reasons for the low environmental impact values. The average reduction rates in CO environmental impact for Jet A1+100 ppm TiO_2 and Jet A1+200 ppm TiO_2 fuels compared to Jet A1 fuel in the 40 k to 120 k rpm range are 9 % and 18 %, respectively. Overall, when evaluating the total environmental impact of HC, NO_x, CO, and CO_2, Jet A1+100 ppm TiO_2 fuel reduces the environmental impact by 1 %, while Jet A1 + 200 ppm TiO_2 fuel increases it by 5 %. The main reason for this result is that Jet A1+200 ppm TiO_2 significantly increases the environmental impact of NO_x at high engine speeds.

Fig. 12 shows the changes in the environmental costs of HC, NO_x, CO, and CO_2 emissions for Jet A1, Jet A1+100 ppm TiO_2, and Jet A1+200 ppm TiO_2 fuels at varying engine speeds. The environmental costs of HC, NO_x, CO, and CO_2 emissions from the jet engine operated at different engine speeds and with various fuels are calculated using the eco-cost of the released exhaust gas products listed in Table 1. When examining the environmental costs of exhaust products emitted from combustion at different speeds and with different fuels, they are ranked from highest to

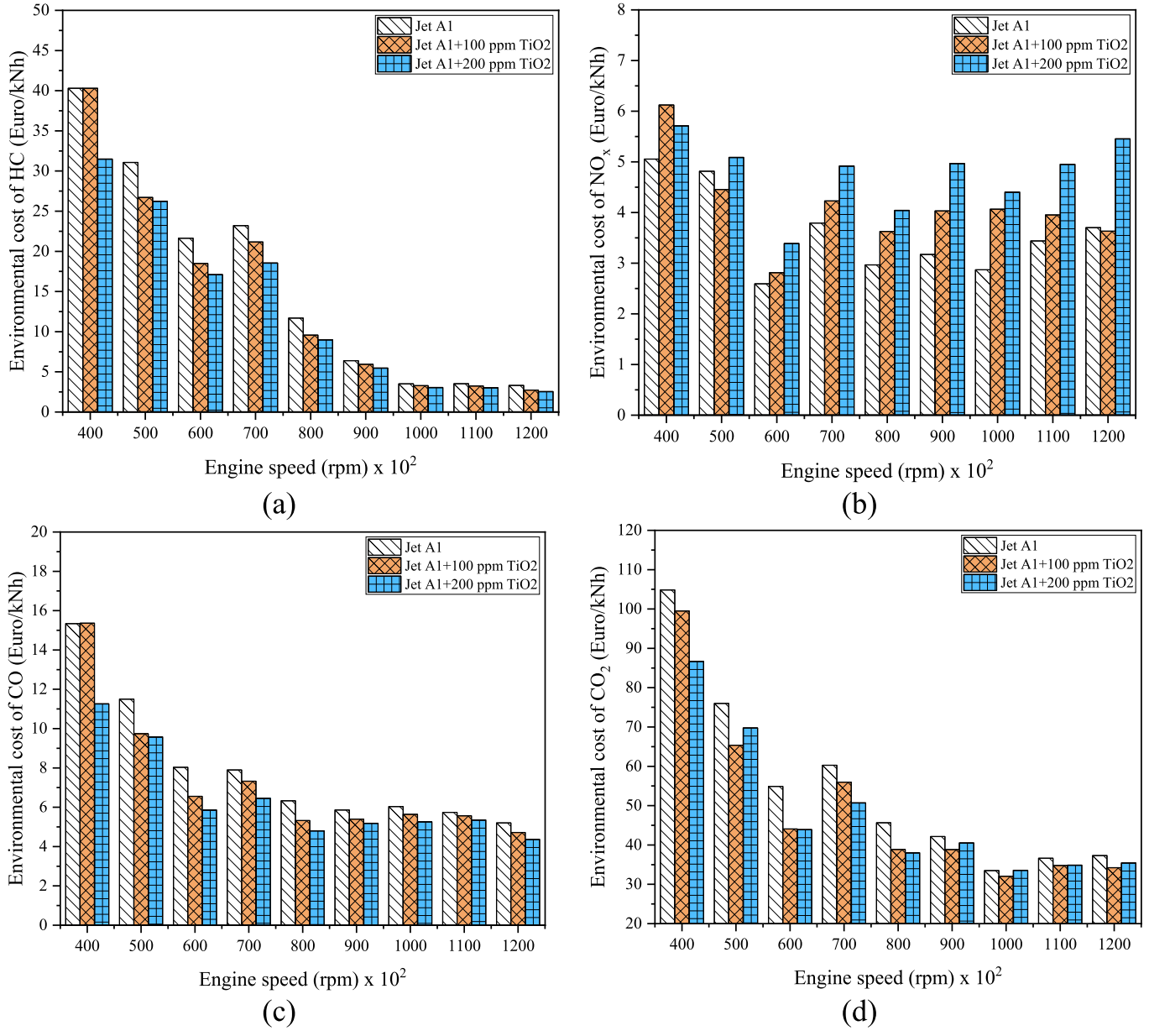

Fig. 12. Variation of environmental cost of (a)HC, (b)NO_x, (c)CO, and (d)CO_2.

lowest as CO_2, HC, CO, and NO_x. As seen in Table 1, although the eco-cost values of NO_x and HC are higher compared to CO and CO_2, the environmental costs of CO_2 are higher. This is due to the higher concentration of CO_2. With the change in engine speed from 40 k to 120 k, all environmental costs, except for NO_x, show a decreasing trend. The main reasons for this are that the increased combustion temperatures and air concentration with the change in speed contribute to the improvement of combustion efficiency, leading to a decrease in HC and CO. The decrease in CO_2 environmental costs with changes in speed can be attributed to reduced fuel consumption. The increase in NO_x environmental costs can be attributed to the improvement of the combustion process and the increase in temperatures in the combustion chamber with the change in speed. Additionally, the use of TiO_2 nanoparticles in Jet A1 fuel shows a reduction in the environmental costs of HC, CO, and CO_2 emissions, except for NO_x. The positive effect of TiO_2 nanoparticles on HC, CO, and CO_2 results in a reduction in the environmental costs of these exhaust products. Overall, when evaluating the total environmental costs of HC, NO_x, CO, and CO_2, Jet A1+100 ppm TiO_2 and Jet A1+200 ppm TiO_2 fuels reduce environmental costs by an average of 8 % and 10 %, respectively.

Fig. 13 shows the changes in the enviro-social costs of HC, NO_x, CO, and CO_2 emissions for Jet A1, Jet A1+100 ppm TiO_2, and Jet A1+200 ppm TiO_2 fuels at varying engine speeds. Unlike the other two evaluations, the enviro-social cost impact of HC and CO emissions is more dominant compared to NO_x and CO_2. The significant increase in the enviro-social cost coefficient for CO and HC emissions in Table 4 is a major reason for the increases shown in Fig. 13(a) and (b). Similar to the environmental impact and environmental cost evaluations, the enviro-social cost impacts of HC, CO, and CO_2 emissions decrease with the upward change in engine speed. However, the enviro-social cost impact of NO_x does not follow a decreasing trend due to increased combustion temperatures resulting from the improved combustion phase with engine speed changes. The reason that the enviro-social cost impact of CO_2 is relatively the same as HC and lower than that of CO is because the enviro-social cost coefficient for CO_2 in Table 1 is lower than the others. Overall, when evaluating the total enviro-social costs of HC, NO_x, CO, and CO_2, Jet A1+100 ppm TiO_2 and Jet A1+200 ppm TiO_2 fuels reduce enviro-social costs by an average of 8 % and 12 %, respectively.

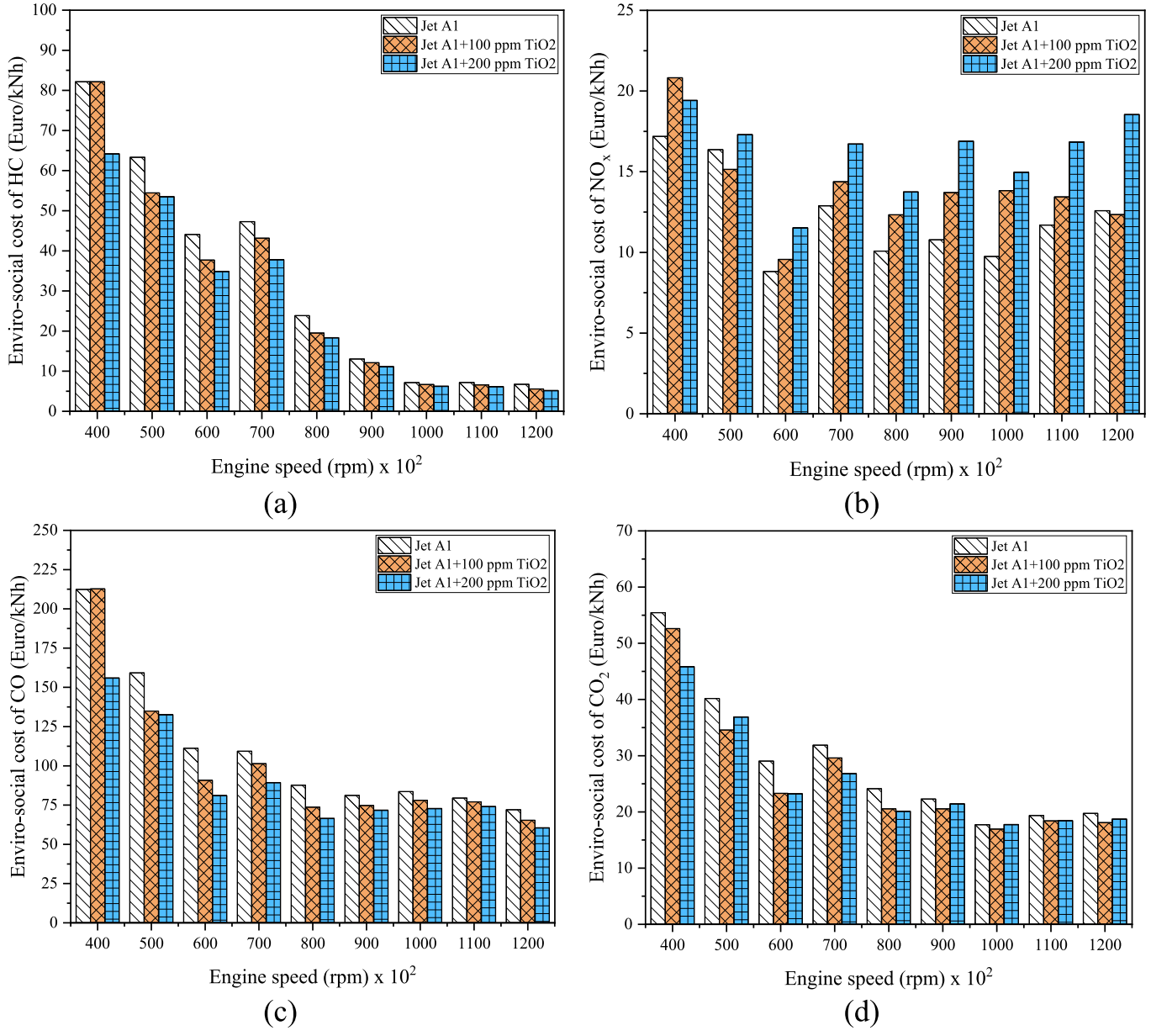

Fig. 13. Variation of enviro-social cost of (a)HC, (b)NO_x, (c)CO, and (d)CO_2.

In the aviation sector, the use of fossil-based fuels contributes to the creation of environmental footprints. The increase in environmental footprints plays a significant role in human health, the environment, and climate change. Furthermore, reducing the spread of emissions into the environment and complying with various regulations incur substantial costs. Therefore, reducing the environmental and economic impacts of emissions is critically important for companies to invest and for the products produced to be commercially viable in the future [68,69].

The use of Jet A1 fuel with TiO_2 nanoparticles in this study contributes to reducing environmental and economic impacts. The use of TiO_2 as an additive in fuels is expected to contribute to reducing carbon-based costs in the coming years and alleviating environmental and economic concerns. Additionally, due to its improvement in fuel consumption, it is anticipated to decrease the use of fossil fuels, thereby reducing both sectoral and individual usage costs.

5. Conclusion

In this study, the effects of adding different proportions of TiO_2 nanoparticles to a kerosene-fueled small jet engine are evaluated in terms of performance, emissions, energy, exergy, environmental impact, enviro-cost impact, and enviro-social cost impact. The conclusions obtained from the analysis and experimental study are as follows:

- TiO_2 nanoparticle additives improve the combustion process by increasing the surface-to-volume ratio, accelerating oxidation activity, and thus contributes to reducing fuel consumption. In the aviation industry, lower fuel consumption results in lower emissions and lower fuel purchasing costs. This situation is more positive from an industrial perspective and encourages the use of TiO_2 in aviation fuels.
- Among the test fuels, the average lowest fuel exergy, combustion chamber exergy destruction, and gas turbine exergy destruction flows are obtained with Jet A1+200 ppm TiO_2 fuel. Compared to Jet A1 fuel, the 200 ppm TiO_2 nanoparticle additive fuel provides reductions of approximately 5 %, 34 %, and 40 % in fuel exergy, combustion chamber exergy destruction, and gas turbine exergy destruction flows, respectively.
- The use of TiO_2 nanoparticles in Jet A1 fuel increases the exergetic efficiencies of the combustion chamber and gas turbine. Jet A1+100 ppm TiO_2 and Jet A1 + 200 ppm TiO_2 fuels increase the exergetic efficiencies of the combustion chamber by an average of 1.8 % and 3.6 %, respectively, compared to Jet A1 fuel. Similarly, they increase the exergetic efficiencies of the gas turbine by an average of 1.9 % and 2.8 %, respectively.
- The use of TiO_2 in jet fuel increases exergetic efficiency, indicating that the fuel is more sustainable, achieves higher efficiency with less fuel, and enhances job potential and energy quality. This allows for more efficient use of available fuels and maximizes benefits. Thus, energy production and usage can be carried out at lower costs.
- Among HC, CO, CO_2, and NO_x emissions, the highest environmental impact is shown by CO_2 emissions, followed by NO and CO emissions. For the three different test fuels, the highest environmental impact is obtained with Jet A1 fuel. The addition of TiO_2 nanoparticles to Jet A1 fuel increases combustion efficiency and reduces fuel consumption, thereby reducing environmental impact values (except for NO_x). Compared to Jet A1 fuel, the average reduction rates in environmental impact for 100 ppm TiO_2 and 200 ppm TiO_2 fuels are 1 % and 5 %, respectively.
- The use of TiO_2 nanoparticles in Jet A1 fuel contributes to reducing the environmental cost impact. Jet A1+100 ppm TiO_2 and Jet A1+200 ppm TiO_2 fuels reduce the total environmental cost impact by an average of 8 % and 10 %, respectively, compared to Jet A1 fuel. When considering the potential for carbon costs to increase in the coming years and the enactment of stricter regulations, reducing the environmental-economic costs with TiO_2 becomes crucial. This situation is believed to play a significant role in raising awareness and enhancing environmental-economic sustainability.

Overall, the use of TiO_2 in Jet A1 fuel contributes to reducing emissions of HC, CO, CO_2, and smoke, except for NO_x emissions. This reduction significantly contributes to lowering the environmental cost impact and the enviro-social cost impact. However, the high environmental impact of NO_x emissions and the increase in NO_x emissions due to TiO_2 nanoparticles reduce the overall environmental benefit. On the other hand, using TiO_2 at a concentration of 200 ppm improves the exergetic efficiencies of jet engine components. It also leads to lower fuel consumption across all engine speeds. Considering the exergy performance and environmental-economic impacts of TiO_2-added fuel, it proves sustainable both in terms of efficiency and cost. This situation holds promise for the aviation sector and industrial activities in the future. The use of TiO_2 as a fuel additive in jet engines is seen as a significant issue due to its contribution to high NO_x emissions. To overcome this issue, the preference may lean towards using low calorific value, high specific heat capacity, and renewable fuels. Additionally, the use of CO_2 gas that does not participate in combustion reactions could be considered for future studies.

CRediT authorship contribution statement

Usame Demir: Writing – original draft, Methodology, Formal analysis. **Halil Erdi Gülcan:** Writing – original draft, Resources, Methodology, Formal analysis. **Salih Özer:** Writing – review & editing, Writing – original draft, Supervision, Methodology, Formal analysis.

Declaration of competing interest

The authors declare that they have no known competing financial interests or personal relationships that could have appeared to influence the work reported in this paper.

Data availability

Data will be made available on request.

References

[1] Yilmaz N, Atmanli A. Sustainable alternative fuels in aviation. Energy 2017;140:1378–86. https://doi.org/10.1016/J.ENERGY.2017.07.077.
[2] Nygren E, Aleklett K, Höök M. Aviation fuel and future oil production scenarios. Energy Policy 2009;37:4003–10. https://doi.org/10.1016/J.ENPOL.2009.04.048.
[3] Barke A, Bley T, Thies C, Weckenborg C, Spengler TS. Are sustainable aviation fuels a viable option for decarbonizing air transport in Europe? an environmental and economic sustainability assessment. Appl Sci 2022;12:597. https://doi.org/10.3390/APP12020597/S1.
[4] Perea-Moreno A-J, Meloni E, Vilardi G, Carlos J, Pires M, Skov IR, et al. Use of sustainable fuels in aviation—a review. Energies 2022;15:2440. https://doi.org/10.3390/EN15072440.
[5] Maroušek J, Itoh S, Higa O, Kondo Y, Ueno M, Suwa R, et al. The use of underwater high-voltage discharges to improve the efficiency of Jatropha curcas L. biodiesel production. Biotechnol Appl Biochem 2012;59:451–6. https://doi.org/10.1002/BAB.1045.
[6] Maroušek J. Use of continuous pressure shockwaves apparatus in rapeseed oil processing. Clean Technol Environ Policy 2013;15:721–5. https://doi.org/10.1007/S10098-012-0549-3/FIGURES/6.
[7] O'Connell A, Kousoulidou M, Lonza L, Weindorf W. Considerations on GHG emissions and energy balances of promising aviation biofuel pathways. Renew Sustain Energy Rev 2019;101:504–15. https://doi.org/10.1016/J.RSER.2018.11.033.
[8] Timko MT, Herndon SC, De La Rosa BE, Wood EC, Yu Z, Miake-Lye RC, et al. Combustion products of petroleum jet fuel, a fischer–tropsch synthetic fuel, and a biomass fatty acid methyl ester fuel for a gas turbine engine. Combust Sci Technol 2011;183:1039–68. https://doi.org/10.1080/00102202.2011.581717.

[9] Gawron B, Białecki T, Janicka A, Suchocki T. Combustion and emissions characteristics of the turbine engine fueled with HEFA blends from different feedstocks. Energies 2020;13:1277. https://doi.org/10.3390/EN13051277.

[10] Hileman JI, Stratton RW. Alternative jet fuel feasibility. Transp Policy 2014;34:52–62. https://doi.org/10.1016/J.TRANPOL.2014.02.018.

[11] Leach F, Kalghatgi G, Stone R, Miles P. The scope for improving the efficiency and environmental impact of internal combustion engines. Transp Eng 2020;1:100005. https://doi.org/10.1016/J.TRENG.2020.100005.

[12] Kalghatgi G. Development of fuel/engine systems—the way forward to sustainable transport. Engineering 2019;5:510–8. https://doi.org/10.1016/J.ENG.2019.01.009.

[13] Kalghatgi G. Is it really the end of internal combustion engines and petroleum in transport? Appl Energy 2018;225:965–74. https://doi.org/10.1016/J.APENERGY.2018.05.076.

[14] Leone TG, Anderson JE, Davis RS, Iqbal A, Reese RA, Shelby MH, et al. The effect of compression ratio, fuel octane rating, and ethanol content on spark-ignition engine efficiency. Environ Sci Technol 2015;49:10778–89. https://doi.org/10.1021/ACS.EST.5B01420/SUPPL_FILE/ES5B01420_SI_001.PDF.

[15] Jiang C, Huang G, Liu G, Qian Y, Lu X. Optimizing gasoline compression ignition engine performance and emissions: combined effects of exhaust gas recirculation and fuel octane number. Appl Therm Eng 2019;153:669–77. https://doi.org/10.1016/J.APPLTHERMALENG.2019.03.054.

[16] Goveas LC, Vidya SM, Vinayagam R, Selvaraj R. Circular bioeconomy approaches for valorizing waste streams into bio-jet. Fuel 2024:361–75. https://doi.org/10.1007/978-981-97-2523-6_15.

[17] Kurzawska-Pietrowicz P, Maciejewska M, Jasiński R. Exhaust emissions from a jet engine powered by sustainable aviation fuel calculated at various cruising altitudes. Combust Engines 2024. https://doi.org/10.19206/CE-186211.

[18] Caranton ARG, Silva V, Galindo M, Pava J, López M, Cerón A, et al. Enhancing performance and emission characteristics of palm based biodiesel blends with aeronautical Additives: A comprehensive analysis in a J69 aviation engine. Energy Convers Manag 2024;313:118600. https://doi.org/10.1016/J.ENCONMAN.2024.118600.

[19] Badami M, Nuccio P, Pastrone D, Signoretto A. Performance of a small-scale turbojet engine fed with traditional and alternative fuels. Energy Convers Manag 2014;82:219–28. https://doi.org/10.1016/J.ENCONMAN.2014.03.026.

[20] Doliente SS, Narayan A, Tapia JFD, Samsatli NJ, Zhao Y, Samsatli S. Bio-aviation fuel: a comprehensive review and analysis of the supply chain components. Front Energy Res 2020;8:499009. https://doi.org/10.3389/FENRG.2020.00110/BIBTEX.

[21] Connelly EB, Colosi LM, Clarens AF, Lambert JH. Risk analysis of biofuels industry for aviation with scenario-based expert elicitation. Syst Eng 2015;18:178–91. https://doi.org/10.1002/SYS.21298.

[22] Braun-Unkhoff M, Riedel U. Alternative fuels in aviation. CEAS Aeronaut J 2015;6:83–93. https://doi.org/10.1007/S13272-014-0131-2/FIGURES/10.

[23] Rye L, Blakey S, Wilson CW. Sustainability of supply or the planet: a review of potential drop-in alternative aviation fuels. Energy Environ Sci 2010;3:17–27. https://doi.org/10.1039/B918197K.

[24] Staples MD, Malina R, Suresh P, Hileman JI, Barrett SRH. Aviation CO_2 emissions reductions from the use of alternative jet fuels. Energy Policy 2018;114:342–54. https://doi.org/10.1016/J.ENPOL.2017.12.007.

[25] Ahmadi MH, Ghazvini M, Nazari MA, Ahmadi MA, Pourfayaz F, Lorenzini G, et al. Renewable energy harvesting with the application of nanotechnology: A review. Int J Energy Res 2019;43:1387–410. https://doi.org/10.1002/ER.4282.

[26] Akl S, Elsoudy S, Abdel-Rehim AA, Salem S, Ellis M. Recent advances in preparation and testing methods of engine-based nanolubricants: a state-of-the-art review. Lubr 2021;9:85. https://doi.org/10.3390/LUBRICANTS9090085.

[27] Vigneswaran R, Balasubramanian D, Sastha BDS. Performance, emission and combustion characteristics of unmodified diesel engine with titanium dioxide (TiO2) nano particle along with water-in-diesel emulsion fuel. Fuel 2021;285:119115. https://doi.org/10.1016/J.FUEL.2020.119115.

[28] Manigandan S, Sarweswaran R, Booma Devi P, Sohret Y, Kondratiev A, Venkatesh S, et al. Comparative study of nanoadditives TiO_2, CNT, Al_2O_3, CuO and CeO_2 on reduction of diesel engine emission operating on hydrogen fuel blends. Fuel 2020;262:116336. https://doi.org/10.1016/J.FUEL.2019.116336.

[29] Manigandan S, Ponnusamy VK, Devi PB, Oke SA, Sohret Y, Venkatesh S, et al. Effect of nanoparticles and hydrogen on combustion performance and exhaust emission of corn blended biodiesel in compression ignition engine with advanced timing. Int J Hydrogen Energy 2020;45:3327–39. https://doi.org/10.1016/J.IJHYDENE.2019.11.172.

[30] Valihesari M, Pirouzfar V, Ommi F, Zamankhan F. Investigating the effect of Fe_2O_3 and TiO_2 nanoparticle and engine variables on the gasoline engine performance through statistical analysis. Fuel 2019;254:115618. https://doi.org/10.1016/J.FUEL.2019.115618.

[31] Gülcan HE, Erol D, Çelik M, Bayındırlı C. Assessment of trade-off, exergetic performance, and greenhouse gas impact-cost analysis of a diesel engine running with different proportions of TiO_2, Ag_2O, and CeO_2 nanoadditives. Energy 2024;313:133786. https://doi.org/10.1016/J.ENERGY.2024.133786.

[32] Rajpoot AS, Choudhary T, Shukla A, Chelladurai H, Rajak U, Sinha AA. Experimental investigation on behavior of a diesel engine with energy, exergy, and sustainability analysis using titanium oxide (TiO_2) blended diesel and biodiesel. J Enhanc Heat Transf 2024;31:1–17. https://doi.org/10.1615/JENHHEATTRANSF.2024051522.

[33] Ghanati SG, Doğan B, Yeşilyurt MK. The effects of the usage of silicon dioxide (SiO_2) and titanium dioxide (TiO_2) as nano-sized fuel additives on the engine characteristics in diesel engines: a review. Biofuels 2024;15:229–43. https://doi.org/10.1080/17597269.2023.2221882.

[34] Upadhyay N, Kumar K, Kumar Das R, Kumar GS. A thermodynamic approach to energy, exergy, exergoeconomic, enviroeconomic, and sustainability assessments involving an VCR diesel engine employing third-generation biodiesel with TiO_2 NPs and n-heptane. Energy Convers Manag 2024;321:119064. https://doi.org/10.1016/J.ENCONMAN.2024.119064.

[35] Altarazi YSM, Abu Talib AR, Yu J, Tahmasebi A, Yusaf T, Gries E, et al. Analyzing the environmental effect and efficiency of additives and nano-additives with biodiesel blends on aero-engine. Fuel 2025;381:133589. https://doi.org/10.1016/J.FUEL.2024.133589.

[36] Yuvarajan D, Dinesh Babu M, BeemKumar N, Amith KP. Experimental investigation on the influence of titanium dioxide nanofluid on emission pattern of biodiesel in a diesel engine. Atmos Pollut Res 2018;9:47–52. https://doi.org/10.1016/J.APR.2017.06.003.

[37] Örs I, Sarıkoç S, Atabani AE, Ünalan S, Akansu SO. The effects on performance, combustion and emission characteristics of DICI engine fuelled with TiO2 nanoparticles addition in diesel/biodiesel/n-butanol blends. Fuel 2018;234:177–88. https://doi.org/10.1016/J.FUEL.2018.07.024.

[38] Sandhi RS, Chebattina KRR, Sambana NR, Vadapalli S, Pullagura G, Pathem UC. Evaluation of TiO_2 nanoparticles as an additive in diesel-n-butanol - bombax ceiba biodiesel blends for enhance performance and emissions control of a CI engine. Int J Heat Technol 2021;39:1930–6. https://doi.org/10.18280/IJHT.390630.

[39] Jafarmadar S, Amini Niaki SR. Experimental exergy analyses in a DI diesel engine fuelled with a mixture of diesel fuel and TiO_2 nanoparticle. Environ Prog Sustain Energy 2022;41:e13703. https://doi.org/10.1002/EP.13703.

[40] D'Silva R, Binu KG, Bhat T. Performance and emission characteristics of a C.I. engine fuelled with diesel and TiO_2 nanoparticles as fuel additive. Mater Today Proc 2015;2:3728–35. https://doi.org/10.1016/J.MATPR.2015.07.162.

[41] Praveen A, Lakshmi Narayana Rao G, Balakrishna B. Performance and emission characteristics of a diesel engine using Calophyllum Inophyllum biodiesel blends with TiO_2 nanoadditives and EGR. Egypt J Pet 2018;27:731–8. https://doi.org/10.1016/J.EJPE.2017.10.008.

[42] Gadalla MA, Mazen OM, Aboul-Fotouh TM, Ashour FH, Elazab HA. Effect of using nanoparticle-based diesel fuel on enhancement of performance and emissions of diesel engines. Nanosci Nanotechnology-Asia 2020;11:104–18. https://doi.org/10.2174/2210681210666200219112202.

[43] Titanium Dioxide (TiO2) Nanopowder/Nanoparticles, Rutile, High Purity: 99.5+ %, Size: 28 nm n.d. https://nanografi.com/nanoparticles/titanium-dioxide-tio2-nanopowder-nanoparticles-rutile-high-purity-99-5-size-28-nm (accessed February 2, 2025).

[44] Al-Hadhrami LM, Shaahid SM, Al-Mubarak AA, Al-Hadhrami LM, Shaahid SM, Al-Mubarak AA. Jet impingement cooling in gas turbines for improving thermal efficiency and power density. Adv Gas Turbine Technol 2011. https://doi.org/10.5772/22020.

[45] Yucer CT. Thermodynamic analysis of the part load performance for a small scale gas turbine jet engine by using exergy analysis method. Energy 2016;111:251–9. https://doi.org/10.1016/J.ENERGY.2016.05.108.

[46] Akdeniz HY, Balli O, Caliskan H. Energy, exergy, economic, environmental, energy based economic, exergoeconomic and enviroeconomic (7E) analyses of a jet fueled turbofan type of aircraft engine. Fuel 2022;322:124165. https://doi.org/10.1016/J.FUEL.2022.124165.

[47] Balli O. Exergy modeling for evaluating sustainability level of a high by-pass turbofan engine used on commercial aircrafts. Appl Therm Eng 2017;123:138–55. https://doi.org/10.1016/J.APPLTHERMALENG.2017.05.068.

[48] Turan O. Exergetic effects of some design parameters on the small turbojet engine for unmanned air vehicle applications. Energy 2012;46:51–61. https://doi.org/10.1016/J.ENERGY.2012.03.030.

[49] Akdeniz HY. Landing and take-off (LTO) flight phase performances of various piston-prop aviation engines in terms of energy, exergy, irreversibility, aviation, sustainability and environmental viewpoints. Energy 2022;243:123179. https://doi.org/10.1016/J.ENERGY.2022.123179.

[50] Yunus Cengel MB and MK. Thermodynamics An-Engineerin Approach Cengel 8th 2004:1–14.

[51] Bejan A, Tsatsaronis G, Moran M. Introduction to thermal system design. Therm Des Optim 1996:1–37.

[52] Kotas TJ. Exergy method of thermal and chemical plant analysis. Chem Eng Res Des; (United Kingdom) 1986;64:3.

[53] Tsatsaronis G, Morosuk T. Understanding and improving energy conversion systems with the aid of exergy-based methods. Int J Exergy 2012;11:518–42. https://doi.org/10.1504/IJEX.2012.050261.

[54] Gürbüz H, Akçay H, Aldemir M, Akçay İH, Topalcı Ü. The effect of euro diesel-hydrogen dual fuel combustion on performance and environmental-economic indicators in a small UAV turbojet engine. Fuel 2021;306:121735. https://doi.org/10.1016/J.FUEL.2021.121735.

[55] Gülcan HE, Ciniviz M. The effect of pure methane energy fraction on combustion performance, energy analysis and environmental - economic cost indicators in a single-cylinder common rail methane-diesel dual fuel engine. Appl Therm Eng 2023;230:120712. https://doi.org/10.1016/J.APPLTHERMALENG.2023.120712.

[56] Bicer Y, Dincer I. Life cycle evaluation of hydrogen and other potential fuels for aircrafts. Int J Hydrogen Energy 2017;42:10722–38. https://doi.org/10.1016/J.IJHYDENE.2016.12.119.

[57] Meyer L, Tsatsaronis G, Buchgeister J, Schebek L. Exergoenvironmental analysis for evaluation of the environmental impact of energy conversion systems. Energy 2009;34:75–89. https://doi.org/10.1016/J.ENERGY.2008.07.018.

[58] Petrakopoulou F, Tsatsaronis G, Morosuk T, Paitazoglou C. Environmental evaluation of a power plant using conventional and advanced exergy-based methods. Energy 2012;45:23–30. https://doi.org/10.1016/J.ENERGY.2012.01.042.
[59] Wang X, Zhang Y, Karthikeyan C, Boomadevi P, Maroušek J, Nasif O, et al. Role of injection pressure on fuel atomization and spray penetration on the Thevetia peruviana and Jatropha curcas biodiesel blends with nanoparticle. Fuel 2022;324:124527. https://doi.org/10.1016/J.FUEL.2022.124527.
[60] Shen T, Wu Y, Alahmadi TA, Alharbi SA, Maroušek J, Xia C, et al. Assessment of combustion and acoustic characteristics of scenedesmus dimorphus blended with hydrogen fuel on internal combustion engine. J Energy Resour Technol Trans ASME 2023;145. https://doi.org/10.1115/1.4056446/1153553.
[61] Shao D, Al Obaid S, Alharbi SA, Maroušek J, Sekar M, Gunasekar P, et al. Prediction of the fuel spray characteristics in the combustion chamber with methane and TiO_2 nanoparticles via numerical modelling. Fuel 2022;326:124820. https://doi.org/10.1016/J.FUEL.2022.124820.
[62] Pulkrabek WW. Engineering fundamentals of the internal combustion engine 2004:478.
[63] Heywood JB. Internal combustion engine fundamentals 1988:930.
[64] Mei N, Zhu VX, Song Hu-Guo-Dong ZH. Soot formation, oxidation and its mechanism in different combustion systems and smoke emission pattern in DI diesel engines. SAE Tech Pap 1991. https://doi.org/10.4271/910230.
[65] Rastogi PM, Sharma A, Kumar N. Effect of CuO nanoparticles concentration on the performance and emission characteristics of the diesel engine running on jojoba (Simmondsia Chinensis) biodiesel. Fuel 2021;286:119358. https://doi.org/10.1016/J.FUEL.2020.119358.
[66] Kalaimurugan K, Karthikeyan S, Periyasamy M, Mahendran G, Dharmaprabhakaran T. Experimental studies on the influence of copper oxide nanoparticle on biodiesel-diesel fuel blend in CI engine. Energy Sources, Part A Recover Util Environ Eff 2023;45:8997–9012. https://doi.org/10.1080/15567036.2019.1679290.
[67] Fayad MA, Sobhi M, Chaichan MT, Badawy T, Abdul-Lateef WE, Dhahad HA, et al. Reducing soot nanoparticles and NOX emissions in CRDI diesel engine by incorporating TiO_2 nano-additives into biodiesel blends and using high rate of EGR. Energies 2023;16:3921. https://doi.org/10.3390/EN16093921.
[68] Akbari M, Loganathan N, Tavakolian H, Mardani A, Streimikiene D. The dynamic effect of micro-structural shocks on private investment behavior. Acta Montan Slovaca 2021;26:1–17. https://doi.org/10.46544/AMS.V26I1.01.
[69] Pavolová H, Bakalár T, Kyšeľa K, Klimek M, Hajduová Z, Zawada M. The analysis of investment into industries based on portfolio managers. Acta Montan Slovaca 2021;26:161. https://doi.org/10.46544/AMS.V26I1.14.